AN ABSTRACT OF THE THESIS OF

JAMES MAXWELL DONALLY for the DOCTOR OF PHILOSOPHY
(Name) (Degree)

in PHYSICS presented on 11 July 1973
(Major) (Date)

Title: MEASUREMENT OF THE HALL COEFFICIENT OF LIQUID SOLUTIONS OF THALLIUM-TELLURIUM

Redacted for Privacy

Abstract approved: _____
Dr. Melvin Cutler

Measurements are made of the conductivity and Hall mobility of liquid solutions of thallium-tellurium, in compositions ranging from pure tellurium to 69.0 atomic percent thallium. At compositions on the thallium-rich side of intrinsic composition (66.7 atomic percent thallium) both the conductivity and Hall mobility are temperature independent, and the data can be explained by existing theories pertinent to diffusive transport in disordered systems. On the tellurium-rich side of intrinsic composition, the Hall mobility is temperature independent whereas the conductivity shows a strong temperature dependence. This behavior is at variance with the theory most relevant to liquid thallium-tellurium mixtures. At intrinsic composition, the Hall mobility shows a moderate temperature dependence, and the data can be explained in light of a two band model.

Measurement of Hall Coefficient of Liquid Solutions of Thallium-Tellurium

by

James Maxwell Donally

A THESIS

submitted to

Oregon State University

in partial fulfillment of
the requirements for the
degree of

Doctor of Philosophy

June 1974

APPROVED:

Redacted for Privacy

Professor of Physics

in charge of major

Redacted for Privacy

Chairman of Department of Physics

Redacted for Privacy

Dean of Graduate School

Date thesis is presented 11 July 1973

Typed by Clover Redfern for James Maxwell Donally

TABLE OF CONTENTS

LIST OF TABLES

LIST OF FIGURES

MEASUREMENT OF THE HALL COEFFICIENT OF LIQUID SOLUTIONS OF THALLIUM-TELLURIUM

I. INTRODUCTION

Conventional transport theory for electrons in crystalline metals and semiconductors assumes that electrons can be treated as independent particles, and that the mean free path of the electrons is large compared to the deBroglie wavelength. Disorder in a lattice causes scattering of electrons, and the mean free path of an electron in a disordered system may be comparable to its deBroglie wavelength. For this reason, conventional transport theory is open to question, and, up until the last ten years, disordered systems have been poorly studied.

In 1960 there appeared in the literature a review article by Ioffee and Regel which reviewed work on disordered semiconductors up to that time (1). Most of the work described in the review article has been on Seebeck and resistivity measurements of liquid systems that show activation energies characteristic of semiconductors. Seebeck and resistivity measurements of liquid solutions of thallium and tellurium have been made by Cutler and Mallon in which the experimental results showed that these solutions could be characterized as semiconductors (2). Furthermore, these measurements seemed to indicate that conventional transport theory could be used

to describe the electronic behavior of these solutions even though it is unlikely that the mean free path of the electrons in the disordered system would be much longer than the deBroglie wavelength. To learn more about the thallium-tellurium system, it was decided that Hall measurements should be made to determine the volume density of carriers.

Early Hall measurements on liquid metals by other investigators gave widely varying results and the accuracy of these measurements was limited. In recent years, some careful Hall measurements have been made on liquid metals. A paper by A. J. Greenfield reports a technique for measuring Hall coefficients of liquid metals, and contains a good summary of results obtained by other experimentalists up to that time (3). In 1964, the time of Greenfield's paper, the reliability of making Hall measurements had improved considerably and the Hall coefficient for a number of pure liquid metals was found experimentally by most investigators to be within 10% of that which would be expected for free electron behavior. In this present work on thallium-tellurium (Tl-Te), it was assumed originally that Hall coefficients would yield accurate values for volume densities of carriers.

The first measurements of the Hall coefficient by this group were done on a sample of 31 atomic percent thallium. At this time the work of J. E. Enderby in England alerted us to the possibility that the Hall coefficient might be negative for this mixture even though the

Seebeck coefficient was found by Cutler and Mallon to be positive. Enderby's work with a number of other liquid semiconductors showed that this is a very general phenomenon (16). A careful check of the sign indeed showed that the Hall coefficient was negative. A negative Hall coefficient suggests that the carriers are electrons, and a positive Seebeck coefficient suggests that the carries are holes. The disagreement between signs cast doubt on the validity of using either the Seebeck or Hall coefficients as indicators of the type of carrier present in the sample. As a result of this anomaly, the emphasis of the project was changed. Further measurements were made in order to cast some light on the nature of the Hall coefficient rather than use the Hall coefficient as a means of measuring the volume density of carriers.

Hall measurements were made at first on mixtures in the p-region as determined by $X < 66.7$.[1/] These measurements yielded Hall mobilities that showed no temperature dependence, but which increased in magnitude as the mixtures became more thallium rich. Similar behavior in semiconducting glasses was reported by B. T. Kolomiets (4). The glasses showed a negative Hall coefficient and a positive Seebeck coefficient. The resistivity of these glasses varied over ten orders of magnitude (depending on composition) but the Hall mobility of all these samples was about the same in magnitude as those in Tl-Te. A. H. Clark measured a negative Hall coefficient for

---

[1/] X66.7 means 66.7 atomic percent thallium, and will be synonymous with $X = 66.7$.

amorphous germanium with a positive Seebeck coefficient (5). (The germanium was prepared by vacuum depositing in on pyrex.) It was apparent that there was a similarity between these other amorphous systems and our own, and that any theory explaining their behavior might yield an explanation of our own.

Measurements were then made in the intrinsic region (X = 66.7) to determine whether or not a singularity exists in the Hall mobility. (At composition X66.7 the Seebeck coefficient changes sign and the resistivity shows a sharp peak.) At the intrinsic composition it was found that the Hall mobility shows a temperature dependence unlike that which is found in the p-region. For X66.7 it was found that the Hall mobility decreases in magnitude with increasing temperature.

Finally, measurements were made in the n-region (X > 66.7). In this region any thallium in excess of concentration Tl_2Te can be regarded as fully ionized (according to work done by Cutler and Field (6)) and Hall measurements would be more likely to be an accurate measure of electron concentration. Such information could possibly be helpful in understanding the liquid thallium tellurium system over the whole range of composition. The Hall mobility for samples in the n-region turned out to be nearly an order of magnitude smaller than the Hall mobility for samples in the p-region; furthermore, the n-region showed no temperature dependence for the Hall mobility and neither did samples in the p-region.

II. EXPERIMENTAL METHOD

General Method

Oven, Magnet, and Overall Configuration of Apparatus

In order to measure the Hall coefficient of a liquid at high temperature it is necessary to mount the cell in which the measurement is made in an oven. The oven and cell in turn must be mounted between the pole faces of a magnet. Since thallium and tellurium have poisonous vapors at the experimental temperatures, the cell and its ancillary clamping equipment is enclosed in a fused quartz envelope. For additional safety the whole apparatus including oven and magnet are surrounded by a hood-like enclosure. The experimental arrangement of the magnet, oven, and cell envelope is shown in Figure 1. An electromagnet with a 6 inch gap, 6 inch pole faces, and a maximum field strength of 5 KG is used. The furnace (tubular in general shape) is insulated in all regions except along the axis of the magnet's pole faces. There, insulation is lacking so that the furnace may sit between the magnet's pole faces. Water cooling of the oven helps to keep the furnace from delivering excess heat to the magnet.

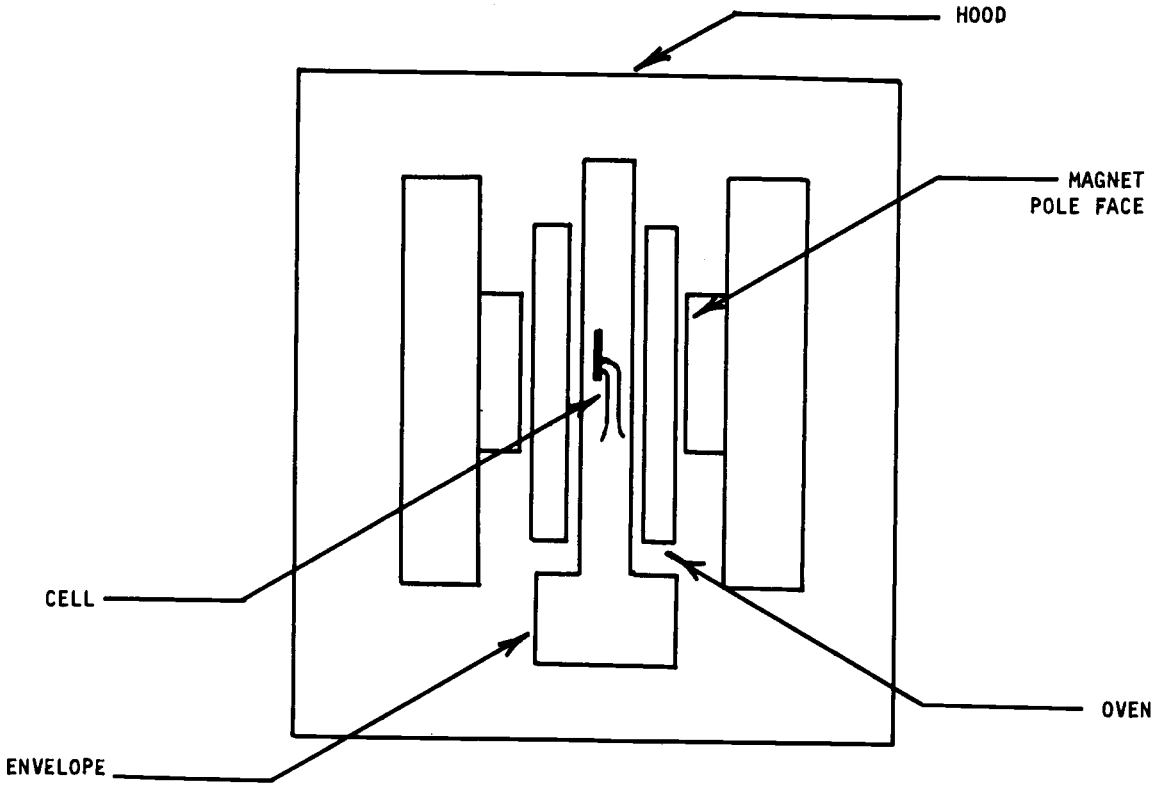

Figure 1. General layout.

Hall Cell

The cell, depicted in Figure 2, is made of quartz. Quartz is used because it is impervious to attack by hot thallium-tellurium, it keeps its strength at the temperatures used in data runs, and because cells can be fabricated from it using standard glassworking techniques. The cell is made up of two plates which are clamped together. One plate (the tube plate) has a quartz tube attached to its face, and the bore of the tube penetrates the thickness of the plate. The tube has a ninety degree bend in it; the bend forms an elbow close to the face of the plate and serves as a reservoir to hold the sample. The tube plate also has five small diameter holes (probe holes) bored in its face. The other plate, shown in Figure 2, has a shallow rectangular trough cut in its face.

Prior to making a run, the dry solid sample is placed in the elbow, heated above the melting temperature, and is mixed to uniformity by gently rocking the cell along its long axis. The liquid sample is then forced by argon gas pressure into the thin channel of the channel plate and beyond that into the five small diameter holes of the tube plate. The thin sheet of liquid in the channel is oriented perpendicular to the magnetic field. The five probe holes, when filled with the liquid, provide lead connections to the circuit. The holes are capped tightly by 1/8" diameter copper-plated graphite pucks.

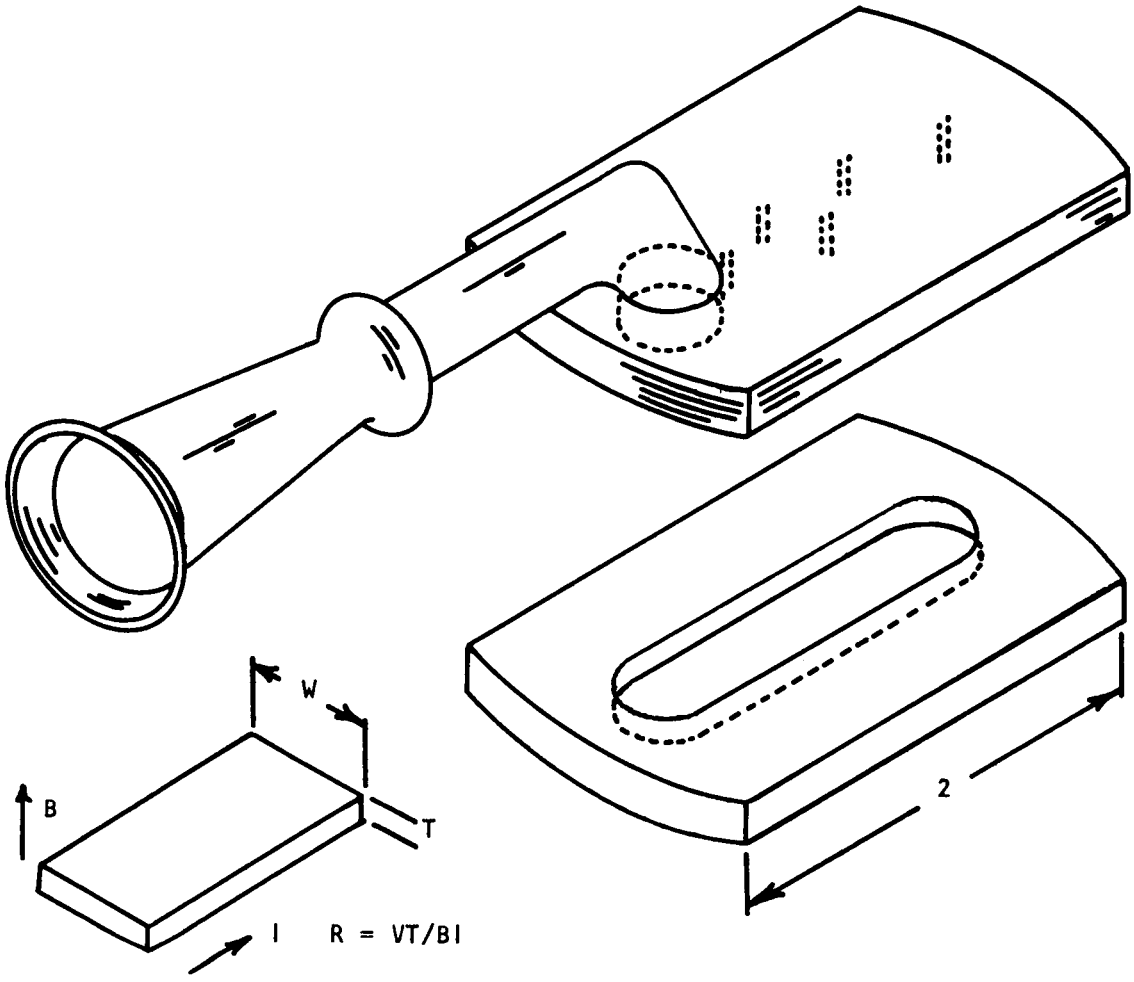

Figure 2. The Hall cell.

Graphite is used because it conducts electricity adequately and is impervious to attack by the sample. The pucks are copper-plated in order to reduce electrical pickup.

The design of the Hall cell is described in detail in Appendix A.

Clamping

In order to clamp the cell together at high temperatures, the cell must be held by springs which retain their strength at these temperatures. Furthermore, the clamping force should be distributed evenly over the faces of the plates. Thin molybdenum ripple springs come in actual contact with the surface of the quartz and they exert the clamping force evenly over the quartz. Tungsten coil springs provide the main clamping force on the quartz plates. A ceramic palette comes between the tungsten springs and the clamped cell. The palette's purpose is multifold, but as far as clamping function is concerned, the palette just provides a flat surface on which the tungsten coil springs can transmit their force evenly to the ripple springs. See Appendix B for further description of the clamping arrangement.

Electrical Measurement

A phase sensitive lock-in amplifier (LIA, Princeton Applied Research Model JB5) is used to eliminate a number of spurious

signals. The reference voltage is taken from a resistor through which the current passes, so that signals out of phase with the current are eliminated. Figure 3 is a block diagram showing how the voltage across the monitoring resistor is measured. In this arrangement an oscillator in the lock-in amplifier controls the power amplifier. Figure 4 shows how a Hall voltage is measured. In this arrangement a three pronged set up is used and a variable resistor is set initially so that zero input comes into the lock-in amplifier. Turning on the magnetic field then generates the Hall voltage which offsets the balance, and that offset is measured as a Hall voltage. Figure 5 shows how the resistivity of the sample is measured. In that arrangement the IR drop down the length of the channel is used to calculate the resistivity. Appendix D has a further description of the electronics.

Special Problems

Leaking

It was found that molten samples of thallium-tellurium readily leaked out of the Hall cells unless special measures were taken. A usual site for leakage was between the cell plates. A special sealing procedure was used which blocked the leak path of the sample and which bonded together the cell plates. It is believed that the presence of thallium oxide absorbed on the quartz surface encourages leaking so

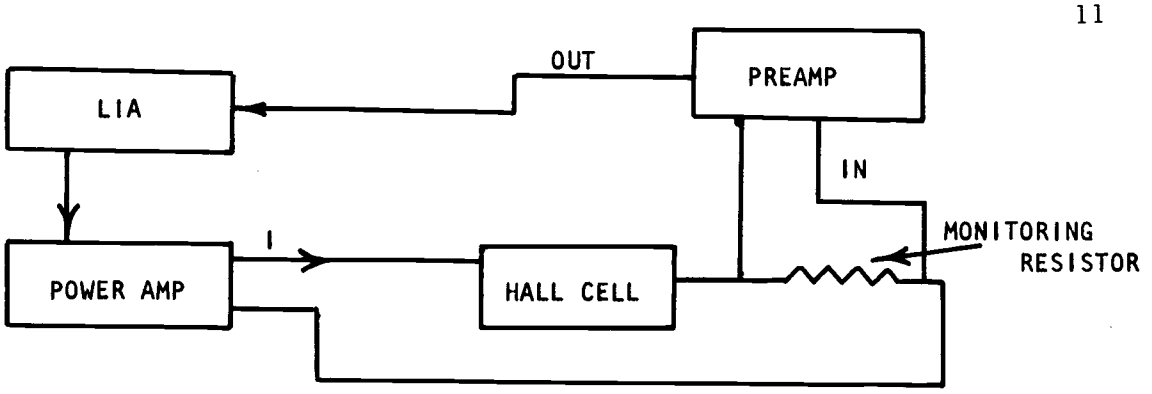

Figure 3. Electronics.

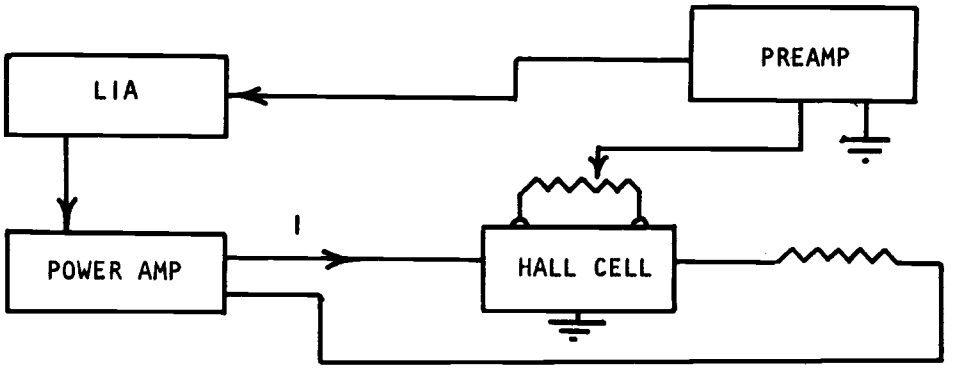

Figure 4. Electronics.

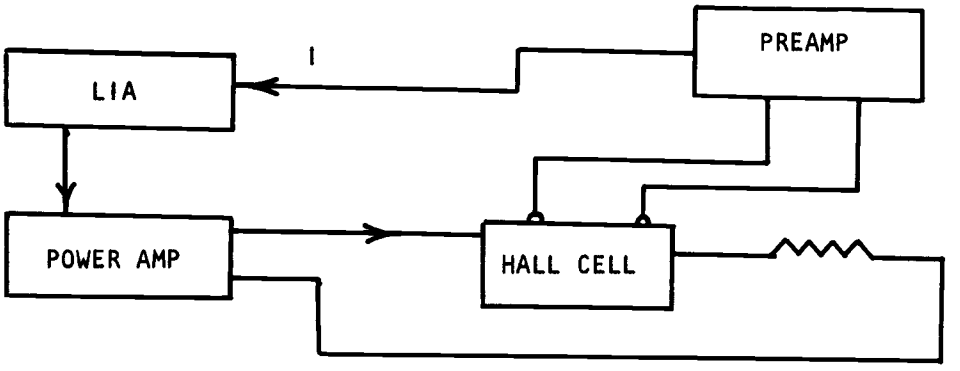

Figure 5. Electronics.

a part of the procedure for preparing samples employs techniques for getting rid of the oxide. The technique for removing oxide from thallium is described in Appendix C.

Vibration of Lead-Out Wires

A spurious signal was found which was traced to vibrations set up by the Lorentz force on the leads carrying the A. C. current in the presence of a magnetic field. This vibrational motion is believed to be transmitted by mechanical coupling to the potential probe leads, whose vibrations in turn, in the magnetic field, cause a spurious voltage because of the Faraday effect. This voltage can have a component in phase with the Hall voltage. Since the current is very large and the Hall voltage is very small, this competing signal could be quite significant.

Convincing evidence that this effect was likely was obtained in a separate experiment carried out at room temperature with a strip of silver playing the role of a sample. The ribbon and its lead-out wires were cemented solidly to a board platform and the platform was placed between the pole faces of the magnet. The signal for the magnetic field going in one direction was equal in magnitude and opposite in polarity from the signal for the magnetic field going in the opposite direction. The magnitude of the signal was such as to give the accepted value for the Hall coefficient of silver. When the same

procedure was repeated with the lead-out wires purposely loosened it was found that for opposite polarity in the magnetic field signals were not necessarily equal in magnitude. However, one-half the absolute value of their difference always yielded the correct value for the Hall coefficient. Similar results were obtained for a similar experiment done on liquid mercury. The magnitude of the spurious signal seemed to depend in a complex or unpredictable way on the frequency of the Hall current, but in all cases for all materials, the correct Hall coefficient was obtained if averaging was done in the above way. Measurements made on mixtures of liquid thallium-tellurium were made with the leads fastened as well as possible and the signal was averaged in the same way as for the mercury and silver.

Drift

A certain amount of drift of the null point can be tolerated, for the results of measurement are recorded on a chart recorder and a first order correction could be made. But occasionally, excessive drift would occur, and efforts were made to eliminate possible causes for the excessive drift. The possible causes are pickup, and bubbles occurring in the sample.

Pickup

In any alternating current experiment there is a danger that wires adjacent to one another can transfer signals and this transfer can cause spurious errors. In any experiment pickup might increase drift. Drift can be caused by a change in coupling due to thermal stresses, so that the pickup signal can be tolerated only by zeroing the balance potentiometer from time to time. Drift rates tended to be higher for higher frequencies of Hall current, and direct evidence of pickup appeared more strongly for higher current frequencies. The direct evidence for pickup came as a change of balance point for the potentiometer as the frequency was increased.

Bubbles

A bubble in the sample can force termination of a data run by causing severe drift or jerkiness in the null point. To minimize the danger of bubbles forming, the following measures were taken:

1. The Hall cell was baked out under vacuum for several hours before filling.
2. The Hall cell was evacuated before filling with the sample. This insured that no gas would be trapped by the sample rushing in. The Hall measurement channel is not sealed against gas leakage, so that if the intended pre-fill vacuum is not

perfect, the residual gas would be likely to be ejected by the incoming sample.

3. The sample was kept at a gauge pressure of about one atmosphere during a run. This pressure would cause any bubbles of (relatively) volatile tellurium oxide to collapse.

Temperature Measurement

Temperature measurement for our cell configuration is difficult because:

1. The oven temperature is far from uniform.
2. Large metal parts extend from the region of the cell to points outside the furnace.
3. The thin channel containing the sample is not conducive to making direct contact between the sample and the thermometer.

When Hall runs were made on p-type samples, it was found that the Hall mobility showed no temperature dependence. Furthermore, accurate data on resistivity vs temperature for various samples existed from measurements made previously by Cutler and Mallon (2) and a reasonable accurate estimate of temperature could be deduced from the sample's resistivity. Approximate measurements could be made by inserting a thermocouple in the general area of the Hall cell.

When Hall runs were made on n-type samples, a much more

accurate means of measuring the temperature was needed. This was necessary because previously made resistivity measurements of n-type samples showed that resistivity was independent of temperature and so temperature could not be inferred from resistivity (6). In order to measure the temperature as accurately as possible, a hole is drilled three quarters of the way into the bottom surface of the channel plate at a spot close to the Hall measuring region of the sample. A thermocouple made of very fine wire (36 gauge) is cemented in the hole. In the bake-out procedure, the cement changes to carbon which provides a good thermal path between the thermocouple wire and the quartz. The fineness of the wire minimizes inaccuracy due to conduction of heat away from the junction. In order to test the accuracy of temperature measurement, temperature vs resistivity readings from the thermocouple were compared with temperature vs resistivity readings done by Cutler and Mallon (2) on an X48 sample, as shown in Figure 6. The measurements of Cutler and Mallon (2) are known to be accurate, and their close agreement with the present work indicates that the present temperature measurements are accurate also.

Validity of the Measurement

The Hall voltage V_H is given by:

$$V_H = R_H \frac{BI}{t}$$

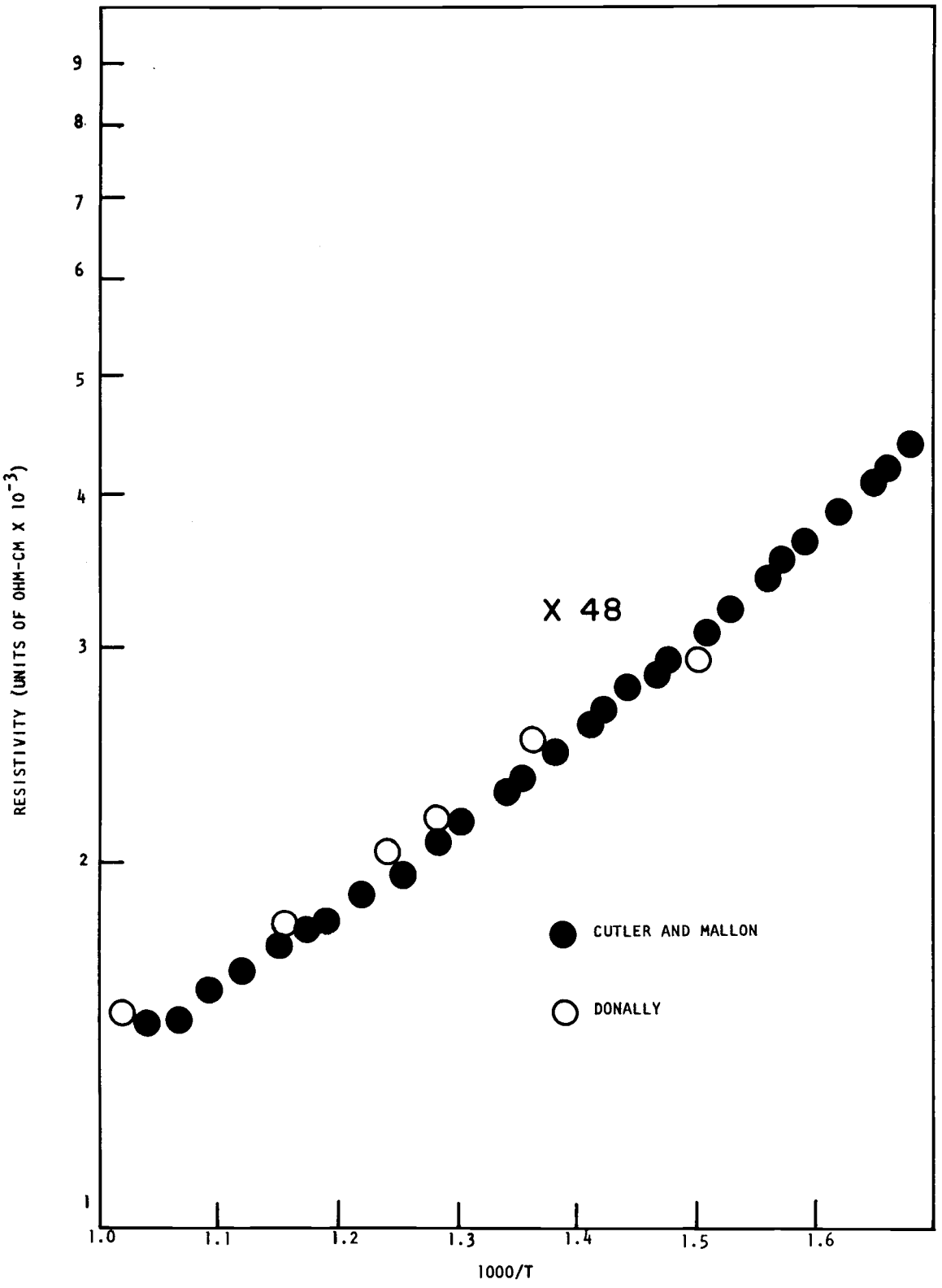

Figure 6 Temperature calibration.

where B is the magnetic field, I is the current, t is the thickness of the cell, and R_H is the Hall coefficient. If alternating current is used, then the Hall voltages are expected to be independent of frequency. Table 1 summarizes the data from a sample of X31 for which the magnetic field is varied while the magnitude of the current is held at a constant value. The table shows the linearity of the voltage through the constancy of V/B at two different frequencies. This result is also illustrated in Figure 7. Table 2 summarizes the data from the same sample in which the magnitude of the current is varied while the magnetic field is held fixed. The table tests the linearity of the voltage in terms of the constancy of V/I. This result is also illustrated in Figure 8. The voltages behave as Hall voltages within the average deviations indicated in the tables. For the measurement of V vs B (I fixed) the overall average deviation was 15% for both frequencies, and for the measurement of V vs I, (B fixed) the overall average deviation for both frequencies was 20%.

Deviations from linearity are believed to be caused by vibrations of the lead-in current-bearing wires. Experiments dealing with vibrating lead-in current-bearing wires are described in the section labeled "Special Problems." The results of the experiments indicated that wires should be fastened down as well as possible. In the actual apparatus, some play in the lead-in wires for X31 was inevitable because of design limitation on the palette. In order to secure every

Table 1. Table of V vs B for I fixed at 1.1 amps.

B(K.G.)	V(μN)	V/B	Deviation from Average (%)
Frequency = 33 cps.			
4.6	5.3	1.1	0
3.7	5.7	1.5	36
2.6	3.1	1.2	8
1.3	1.7	1.3	8
-1.3	-1.4	1.1	0
-2.6	-3.0	1.2	8
-3.7	-2.5	.7	-36
-4.6	-2.9	.6	-45
Average of absolute values of deviations: 18%.			
$V/B_{ave.}$ = 1.1 μV/KG.			
Frequency = 330 cps.			
4.6	4.9	1.5	+25
3.7	5.5	1.5	+25
2.6	3.5	1.3	+ 8
1.3	1.2	.9	-25
-1.3	-1.0	.8	- 7
-2.6	-3.1	1.2	0
-3.7	-3.9	1.1	- 8
-4.6	-5.7	1.2	0
Average of absolute values of deviations: 12%.			
$V/B_{ave.}$ = 1.2 μV/KG			
Overall average deviations for both frequencies: 15%			

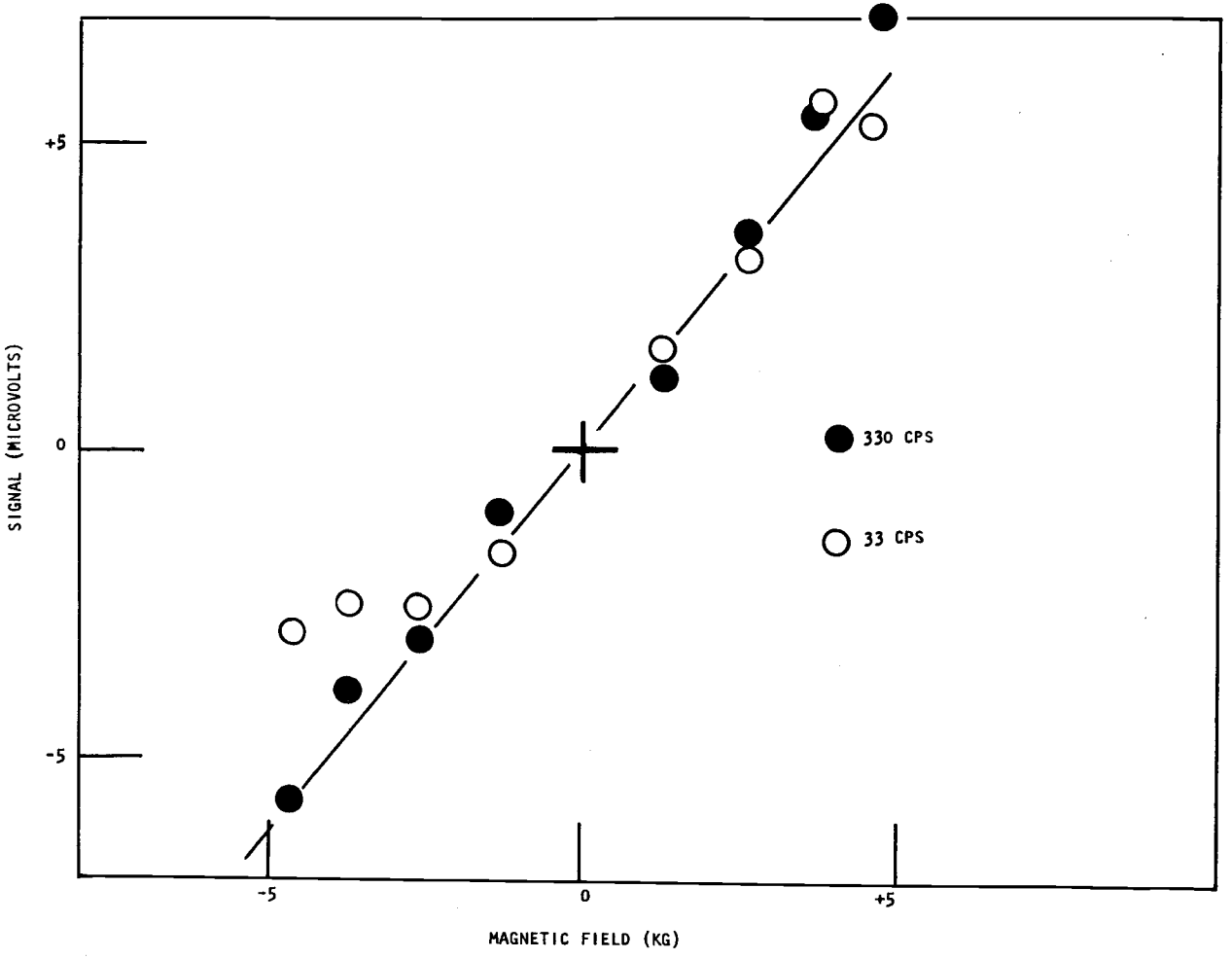

Figure 7. Signal vs field, current fixed.

Table 2. Table of V vs I, B fixed at 4.6 K.G. (then reversed to -4.6 K.G.).

I (amps)	V(+B)(μV)	|V/I|	Deviation from Average (%)
Frequency = 33 cps.			
1.1	6.2	5.6	+19
.83	5.3	6.4	+36
.55	3.1	5.6	+19
.28	1.5	5.4	+15
	V(-B)(μV)		
1.1	-2.4	2.2	-53
.83	-3.1	3.7	-21
.55	-2.2	4.0	-15
.28	-1.2	4.3	- 8

Average of absolute values of deviations: 23%.
$|V/I|_{ave}$ = 4.7 μV/amp.

	V(+B)(μV)		
Frequency = 330 cps.			
1.1	6.9	6.3	+34
.83	4.4	5.3	±13
.55	2.7	4.9	+ 4
.28	1.2	4.3	-10
	V(-B)(μV)		
1.1	-5.7	5.2	+45
.83	-2.2	2.6	-45
.55	-2.6	4.7	0
.28	-1.2	4.3	- 9

Average of absolute values of deviations: 16%.
$|V/I|_{ave}$ = 4.7 μV/amp.

Overall average deviations for both frequencies: 20%.

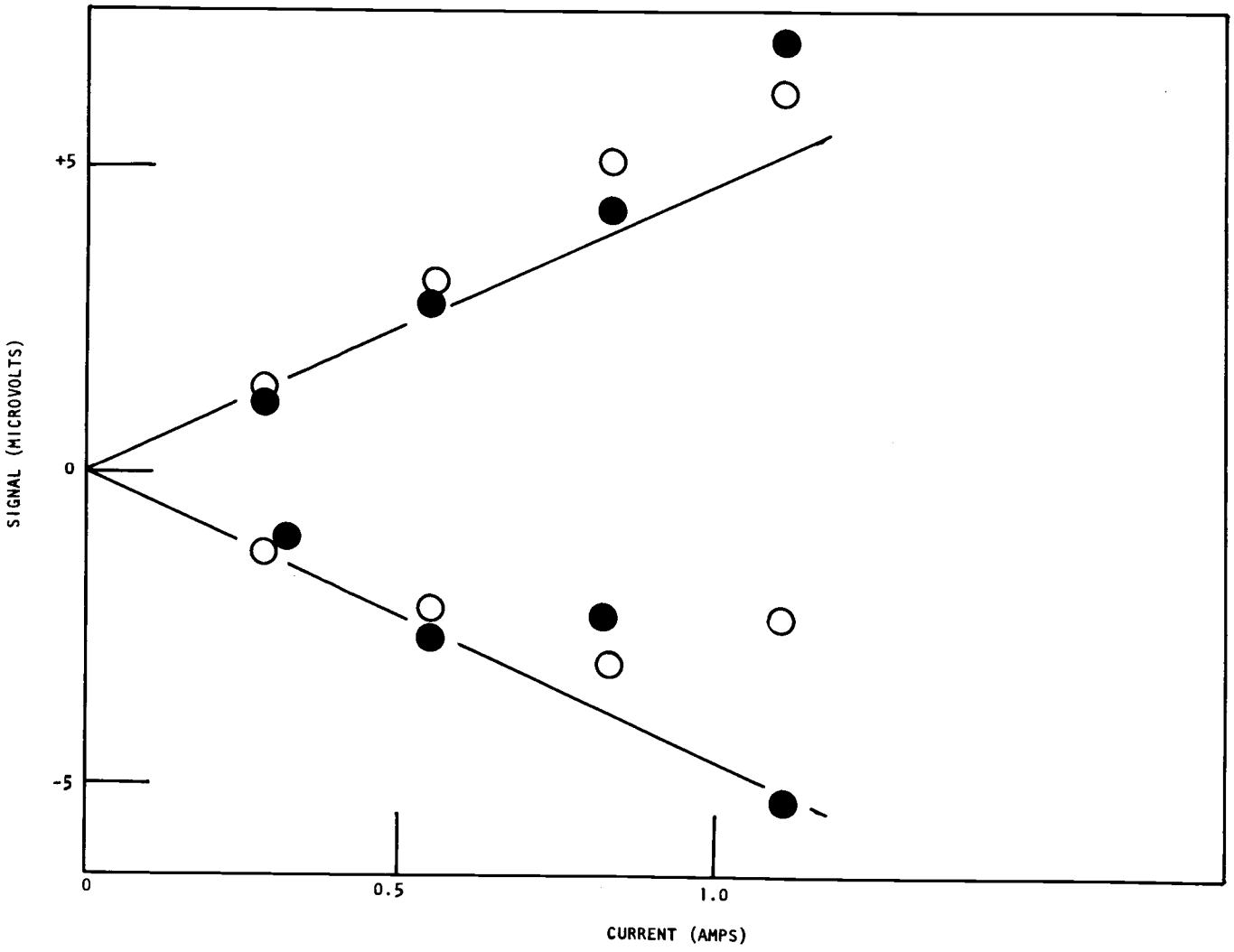

Figure 8. Signal vs current, magnetic field fixed.

inch of lead-in wire, the palette and arbors would have had to have been cemented into a solid piece, and assembly-disassembly of the cell, arbor, and palette would have been impossible.

Although there is some deviation from linearity as seen in the experiments on linearity, there appears to be no significant difference in the average slopes for the different frequencies. This agreement in slope for measurements done at different frequencies indicates that the basic behavior of the voltages is independent of frequency, as is required for Hall voltages.

Measurement of the Hall Coefficient

The Hall coefficient is given by $R_H = V_H tR/V_I B$ where V_H is the Hall voltage, V_I is the IR drop across a monitoring resistor, R, which is in series with the Hall cell. (I is the Hall current through the cell.) B is the strength of the magnetic field, and t is the depth of the channel.

Measurement of B

B is measured with a Radio Frequency Laboratories gauss-meter of 0.1% accuracy. The field which is regularly used is of strength 4.6 KG ± 0.1 KG. The error stated comes from the uncertainty of position of the Hall cell in the pole faces along with small inhomogeneities of the magnetic field.

Measurement of t

The measurement of t, the depth of the channel, is described in Appendix A.

Measurement of R

R was placed in series with a standard resistor (accuracy 0.1%) and an alternating current was passed through both resistors. The IR drops across the two resistors were amplified with a Keithly Model 103 amplifier, and then compared with the use of a Tektronix Model 450 oscilloscope. All attenuating switches were checked. R has a value of 2.50 milliohms ± .05 milliohms providing it passes a current no larger than two amperes peak-to-peak.

Measurement of the Sign of the Hall Coefficient

In order to measure the sign of the Hall coefficient, the direction of the magnetic field was determined by noting the direction of the force it exerted on a current bearing wire. When the field was turned on, the Hall voltage that appeared on a sample of X31 was recorded by the lock-in amplifier. The potentiometer was then adjusted in such a way as to imitate the Hall signal, and the direction of the Hall electric field was thereby established. As an additional check, the polarity of the X31 sample was observed to be the same as

that of samples of silver and mercury which are known to be n-type.

Results

Measurements of Hall mobility vs temperature were made on liquid mixtures of thallium and tellurium.

Measurements were made on p-type mixtures whose compositions ranged from pure tellurium (X0) to 60 atomic percent thallium (X60). For these measurements, the temperature ranged from 340°C to 677°C. Hall mobility vs temperature for these mixtures (X31, X45, X60) are plotted in Figure 9, and the data is tabulated in Tables 3-5. Another set of measurements was made on n-type mixtures whose compositions ranged from 67.3 atomic percent thallium to 69.0 atomic percent thallium. For these measurements, the temperature ranged from 450°C to 677°C. Hall mobility vs temperature for these mixtures (X67.3, X68.0, X69.0) are plotted in Figure 10, and the data is tabulated in Tables 6-8.

For both p-type and n-type mixtures the Hall mobilities are independent of temperature over the temperature range measured, as can be seen in Figures 9 and 10.

For the p-type mixtures, the value of μ_H changes systematically over the range of composition measured. It goes from a value of 0.23 cm^2/v-sec for pure Te to a value of 0.45 cm^2/v-sec for 60 atomic percent thallium, as is seen in Figure 11.

For the n-type mixtures, also shown in Figure 11, the value of μ_H also changes systematically, but it registers a considerably lower value than for the p-type mixtures. It goes from a value of 0.10 cm^2/v-sec for 67.3 atomic percent thallium to 0.12 cm^2/v-sec for 69.0 atomic percent thallium.

Measurements were made on an intrinsic mixture of composition 66.7 atomic percent thallium. Temperature for these measurements ranged from 485°C to 677°C, and the Hall mobility showed a systematic change in value over this temperature range, as is seen in Figure 12. The mobility ranged from a high value of 0.31 cm^2/v-sec at 460°C to a low value of 0.18 cm^2/v-sec at 670°C. This variation of mobility with temperature for X66.7 contrasts with the constant mobility for the n-type and p-type mixtures.

Table 3. Summary of results for X31 (p-type).

T(°C)	T(°K)	1000/T	ρ (units of $10^{-3}\Omega$-cm)	R_H (units of $10^{-3}cm^3$/Coul)	μ (cm^2/v-s)
340	613	1.63	2.40	.79	.33
405	678	1.48	1.69	.58	.34
555	828	1.21	1.17	.36	.31
395	668	1.50	1.67	.53	.32
640	913	1.10	.97	.34	.35

Average $\mu = .33 \pm .01$ cm^2/v-s

Table 4. Summary of results for X45 (p-type).

T(°C)	T(°K)	1000/T	ρ (units of $10^{-3}\Omega$-cm)	R_H (units of $10^{-3}cm^3$/Coul)	μ (cm^2/v-s)
537	810	1.24	2.00	.85	.42
562	835	1.20	1.64	.63	.38
365	638	1.57	2.93	1.24	.39
418	691	1.45	2.38	1.01	.43
533	806	1.24	1.72	.73	.42

Average μ = .41 ± .01 cm^2/v-s

Table 5. Summary of results of X60 (p-type).

T(°C)	T(°K)	1000/T	ρ (units of $10^{-3}\Omega$-cm)	R_H (units of $10^{-3}cm^3$/Coul)	μ (cm^2/v-s)
515	788	1.26	3.42	1.64	.46
550	823	1.22	3.05	1.38	.44
590	863	1.16	2.85	1.30	.45
630	903	1.05	2.72	1.20	.44

Average μ = .45 ± .01 cm^2/v-s

Table 6. Summary of results for X67.3 (n-type)

T(°C)	T(°K)	1000/T	ρ (units of $10^{-3}\Omega$-cm)	R_H (units of 10^{-3} cm^3/Coul)	μ (cm^2/v-s)	% Dev. for μ
522	795	1.26	2.21	.222	.100	4%
563	836	1.20	2.18	.204	.094	1%
599	872	1.12	2.02	.208	.103	3%
639	912	1.10	1.99	.194	.098	5%
677	950	1.03	1.91	1.98	.103	3%

$\bar{\mu}$ = .100 ± .001

Table 7. Summary of results for X68.0.

T(°C)	μ (cm^2/v-s)	A.D. for μ(%)
450	.11	30
500	.08	10
555	.11	7
610	.11	7

$\bar{\mu}$ = .11

Table 8. Summary of results for X69.0 (n-type).

T(°C)	T(°K)	1000/T	ρ (units of $10^{-3}\Omega$-cm)	R_H (units of $10^{-3}cm^3$/Coul)	μ (cm^2/v-s)	% Dev. for μ
535	808	1.24	1.01	.135	.134	6%
565	838	1.19	0.99	.130	.130	3%
604	877	1.14	0.98	.122	.125	0%
639	912	1.10	0.98	.135	.135	7%
677	950	1.05	1.00	.129	.129	2%
514	787	1.27	1.00	.119	.119	5%
545	818	1.22	0.99	.122	.124	2%
582	855	1.17	0.98	.120	.123	2%
617	890	1.12	1.00	.127	.127	0%
655	928	1.08	0.98	.133	.136	8%
517	790	1.26	1.00	.129	.129	3%
563	836	1.20	0.99	.125	.127	0%
602	875	1.14	1.00	.123	.123	2%
634	907	1.10	1.00	.110	.110	10%

$\bar{\mu} = .126 \pm .001$

Table 9. Summary of results for X66.7 (intrinsic). Runs taken June 29 and April 29, 1969.

T(°C)	T(°K)	1000/T	ρ (units of 10^{-3} Ω-cm)	R_H (units of 10^{-3} cm^3/Coul)	μ (cm^2/v-s)	% Dev. for μ
499	772	1.30	10.6	3.20	.300	10
563	836	1.20	7.80	1.62	.208	2
642	915	1.09	4.73	0.91	.194	3
522	795	1.26	10.2	3.06	.300	6
463	736	1.36	15.6	4.84	.309	2
602	875	1.14	6.29	1.18	.186	10
677	950	1.05	3.78	0.72	.189	3
547	820	1.22	8.67	1.95	.224	2
614	887	1.13	5.44	1.11	.204	3
656	929	1.07	4.45	0.83	.185	10
The above data were obtained on 6/29/69.						
485	758	1.32	12.7	3.9	.31	10
535	808	1.24	11.5	2.7	.24	10
605	878	1.14	7.6	1.4	.19	3
520	793	1.26	11.4	1.3	.24	2
670	943	1.06	5.6	1.0	.18	1
The data directly above was obtained on 4/29/69. The current was measured improperly, so the Hall coefficient and resistivity are improper. However, the mobility is proper.						

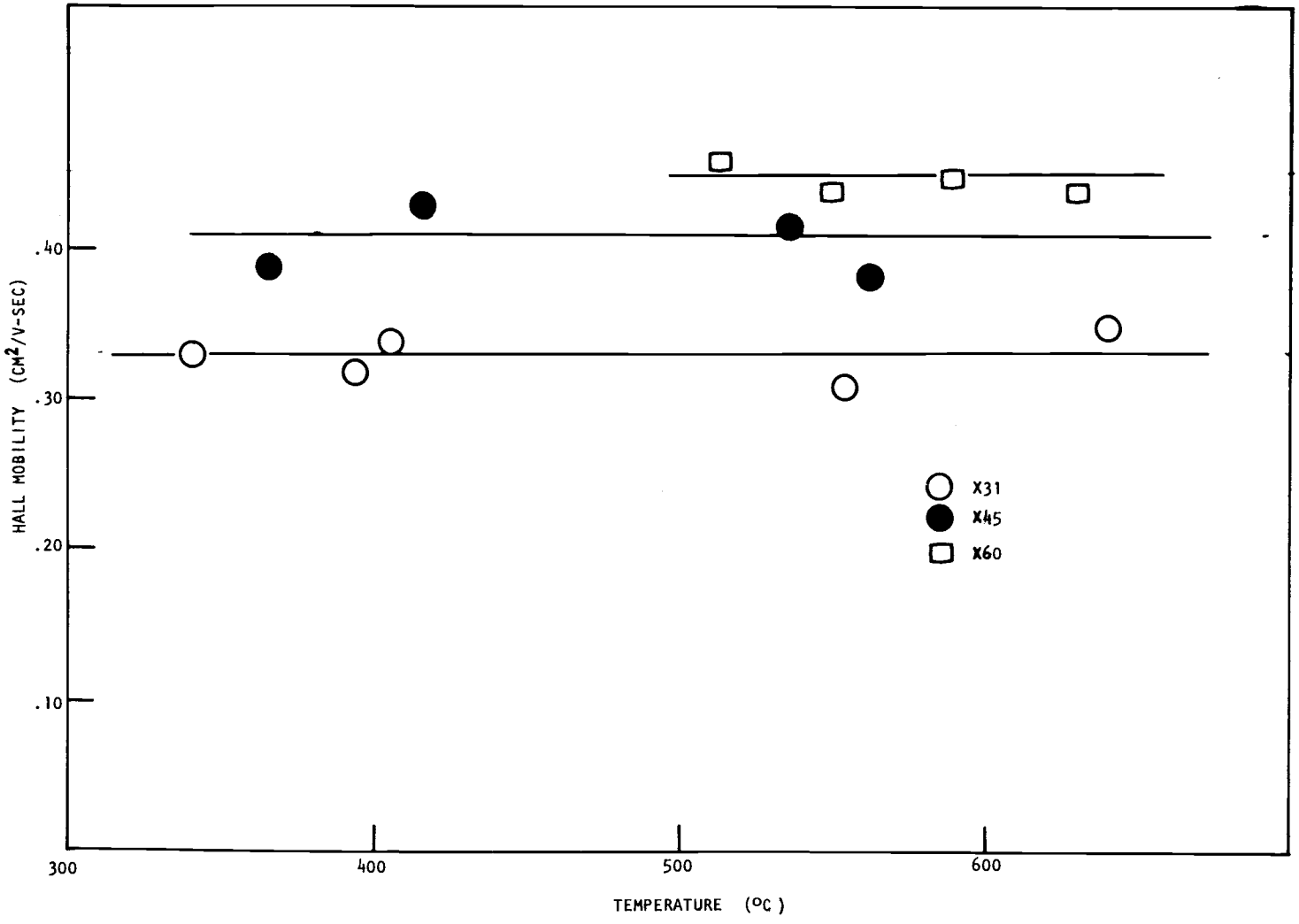

Figure 9. Hall mobility vs temperature in the p-region.

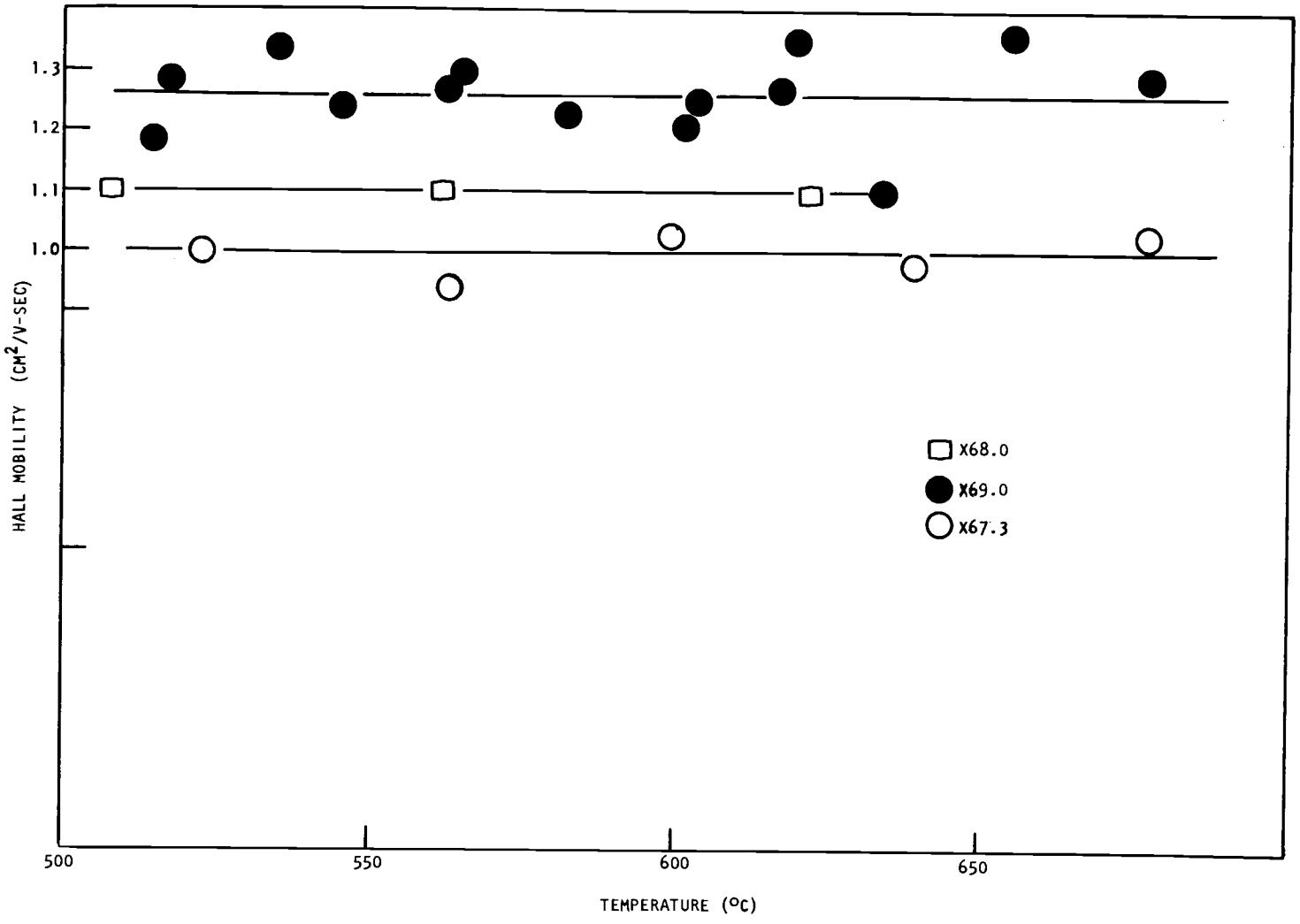

Figure 10. Hall mobility vs temperature in the n-region.

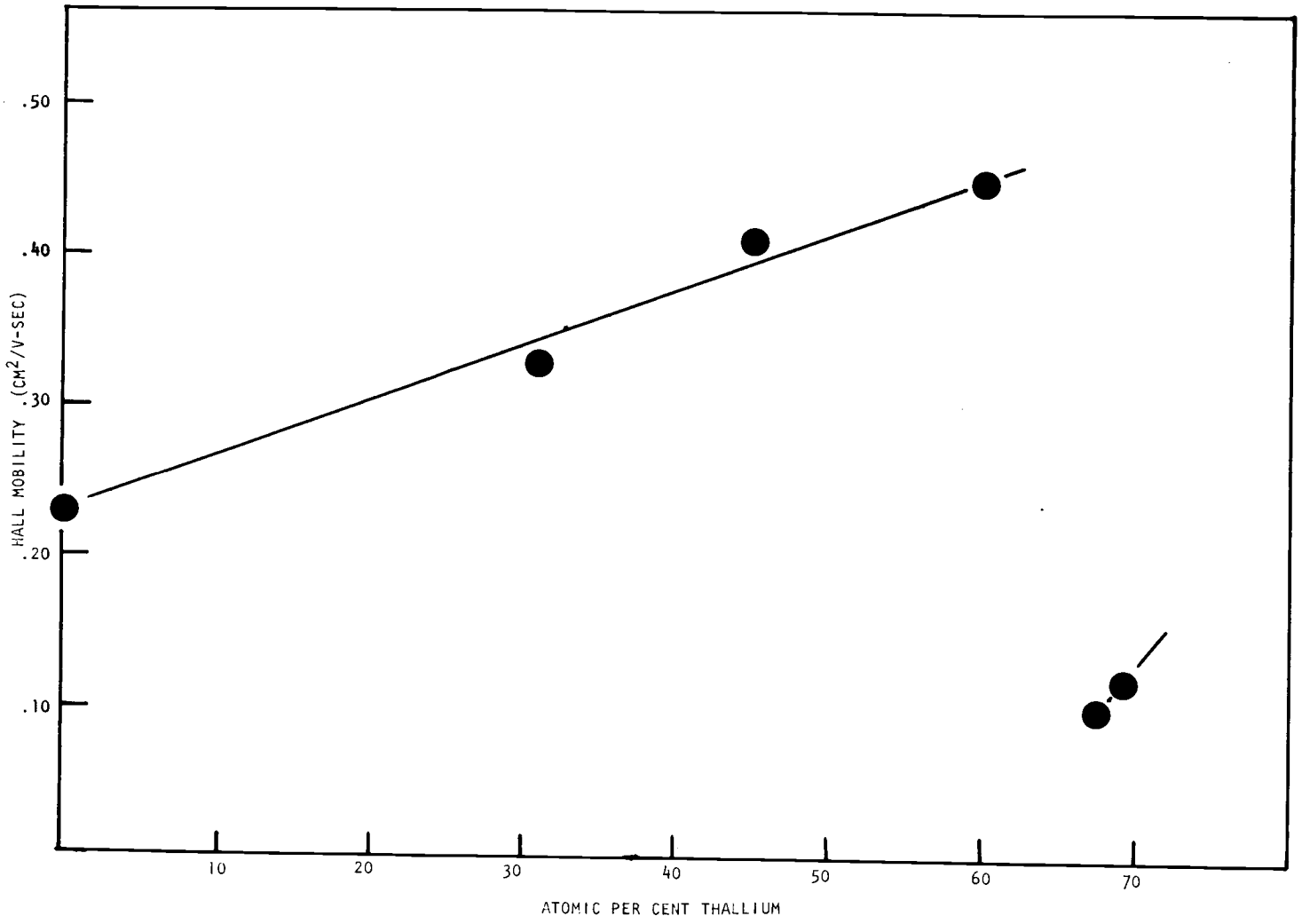

Figure 11. Hall mobility vs composition.

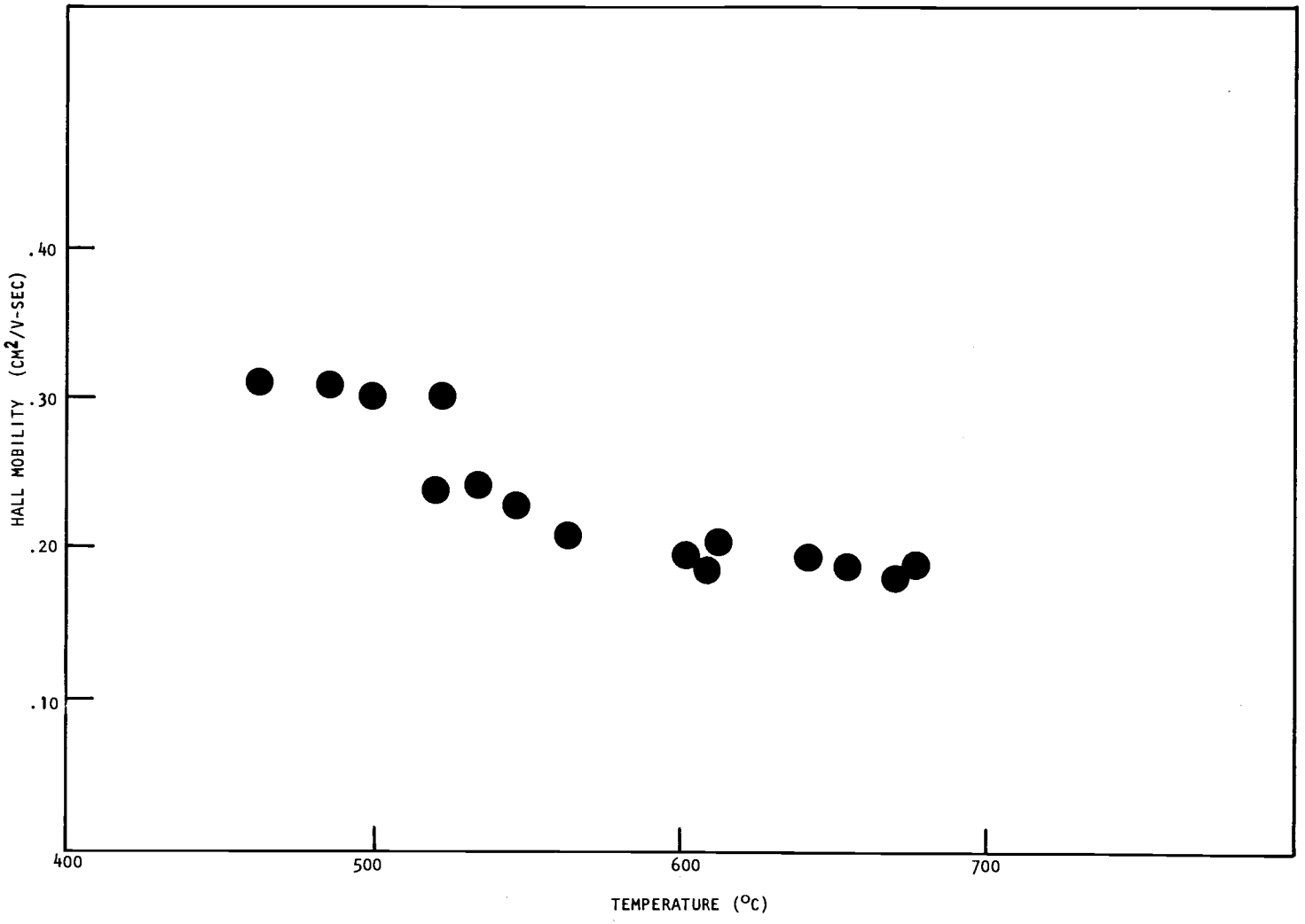

Figure 12. Hall mobility vs temperature in the intrinsic range.

III. DISCUSSION

Relation to Other Work

Work on Other Disordered Systems

Other disordered systems have been studied in which the Seebeck coefficient is positive and the Hall coefficient is negative. Measurements made on chalcogenide glasses show this anomaly (4). There, the resistivity is many orders of magnitude greater than that in the liquid Te-Tl mixtures, but the magnitude of the Hall mobility is in the same range (0.1 cm^2/v-sec - 0.5 cm^2/v-sec) and is similarly temperature independent. A.H. Clark measured a negative Hall coefficient for amorphous germanium with a positive Seebeck coefficient (5). Measurements by Enderby and Walsh (16) on a number of liquid semiconductors show a sign anomaly between the Hall coefficient and Seebeck coefficient. A recent paper by Allgaier (17) gives references to all the Hall measurements made on liquid semiconductors up to the time of publication of the paper.

Recent measurements of the Knight shift and conductivity of liquid tellurium by Warren (7) yield data that shows that the conductivity is proportional to the square of the Knight shift, which is in accordance with a diffusive transport model, applicable to disordered systems (10). Comparison by Warren of the Knight shift with accepted values of the Hall coefficient shows that the Knight shift is close to being inversely proportional to the square of the Hall coefficent. This is at variance with the theory for the Hall coefficient proposed by Friedman (15). It would be inferred from Friedman's calculations

that the Hall coefficient and the Knight shift would be inversely proportional to the first power. This is not observed.

Other Work on Tl-Te

Recently, measurements have been made on tellurium-rich mixtures of Tl-Te by Enderby (8). He plots resistivity vs temperature and Hall coefficient vs temperature. The Hall mobility is computed from these graphs by drawing curves through the resistivity points and Hall points and then computing the appropriate quotient from the curves at each temperature. The Hall mobilities derived in this way from Enderby's data show no regular or systematic temperature dependence. If an average mobility is computed for each composition, then these averages show close agreement with our data when mobility vs composition is plotted (Figure 13)(ref. 8).

Theoretical Interpretation

What Tl-Te is Like on the Basis of Theory and Experiment Unrelated to Hall Measurements

The Pseudogap Theory of Electronic States. The application of the wave equation to conduction electrons in a periodic potential of a crystalline lattice yields wave functions which extend throughout the crystal and which have sharply defined momenta. The phase of the wave functions changes continuously with position as would arise from coherent scattering of an electron by the periodic potential.

When the lattice becomes disordered, the wave functions have

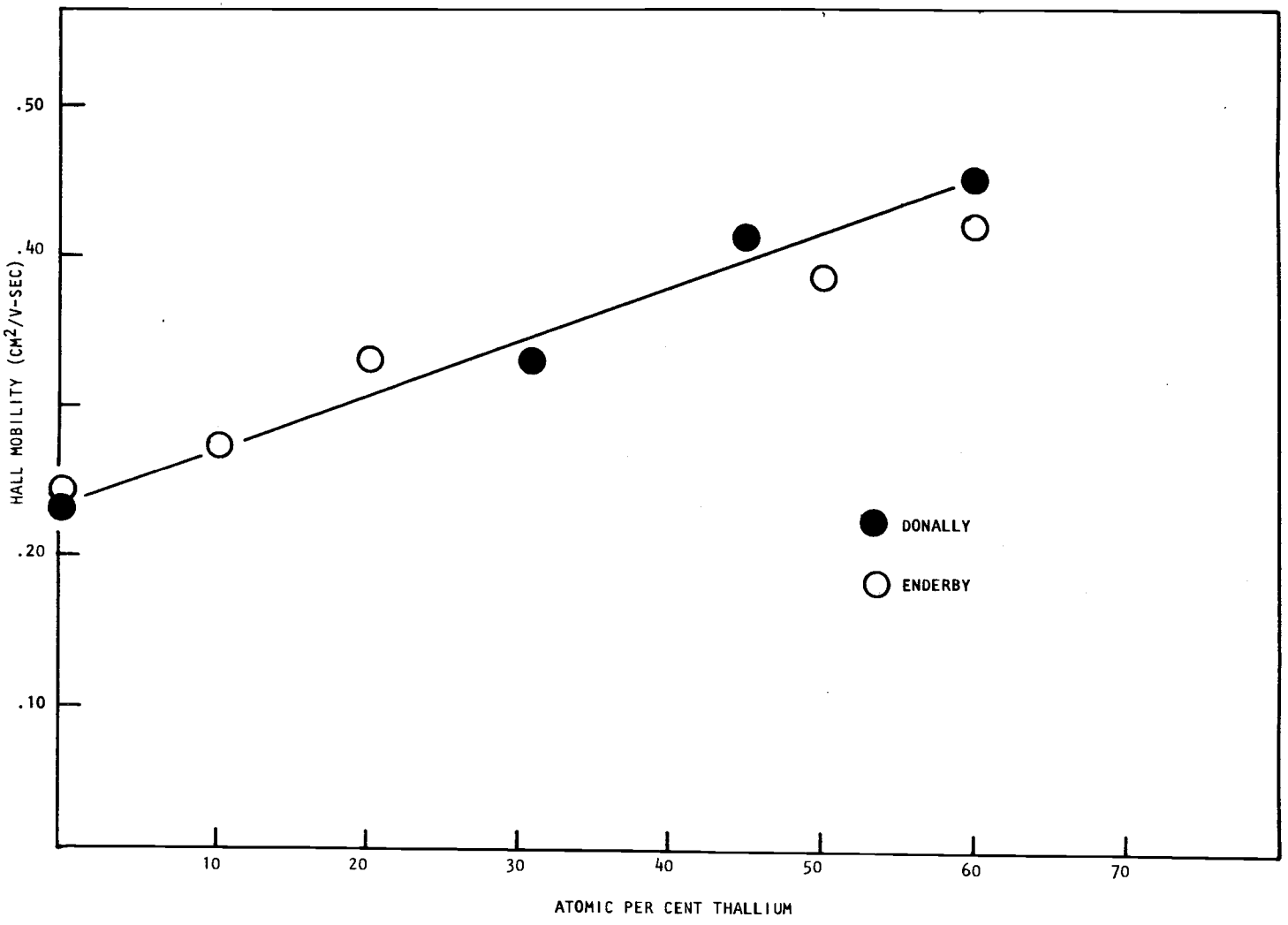

Figure 13. Comparison of Hall mobility results with work of Enderby and Simmons.

large mean deviations for momentum eigenvalues, and the phases add incoherently in scattering from atomic site to atomic site. If the disorder becomes large enough so that the potential fluctuations have a mean value which exceeds the band width by a fixed factor μ (the Anderson criterion) the wave functions become localized (9). The value of μ is difficult to determine precisely, and has a value of approximately 5.

Mott has extended Anderson's result by considering the possibility that some states of the band are localized and others are not (10). By using a metallic model in which the density of states $N(E)$ is reduced in some region of energy as the result of an increased interaction potential between the electrons and the ions, he showed potential fluctuations are expected to cause localization for those energies for which the ratio, g, of $N(E)$ to the free electron value $N^{o}(E)$ falls to a low enough value. Mott estimated the ratio for which localization occurs to be about 1/3. The metallic model may not be a good model for liquid semiconductors or amorphous solids, but his result that there is a sharp boundary between localized and non-localized states is widely accepted.

The region in which $N(E)$ has a minimum is called a pseudogap, and is illustrated in Figure 14. On the basis of a metallic model with strong scattering, Mott has found that at the energy E_c at which localization occurs, the conductivity of the extended states $\sigma(E_c)$ has

a value in the range of 100-300 ohm^{-1}-cm^{-1}. There is a range of energies near E_c with $N(E) > N(E_c)$ in which the non-localized electrons are so strongly scattered that the scattering distance λ is comparable to the interatomic distance a. The upper limit of this range is estimated by Mott to occur when $\sigma(E) \approx 2000$ ohm^{-1}-cm^{-1}. This range of electrical conductivities where strong scattering occurs is called the diffusive range, and it encompasses the experimental domain for liquid Tl-Te.

Figure 14 shows a pseudogap with localized states at the center of the gap, and separated from the extended states on both sides by E_c. Conductivity can be from both extended and localized states, and the extent of the contribution from each depends on the position and width of df^o/dE, f^o being the unperturbed fermi function. ($\sigma = \int \sigma df^o/dE \, dE$ (ref. 6).) Figure 15 shows conduction purely from localized states with df^o/dE narrow, and in the middle of the pseudogap. Figure 16 shows conduction from both localized and extended states, with df^o/dE extending its tail into the non-localized conduction region. Figure 17 shows conduction from extended states, with the fermi energy well away from the pseudogap. For the case shown in Figure 15 when both localized and non-localized states contribute to conductivity,

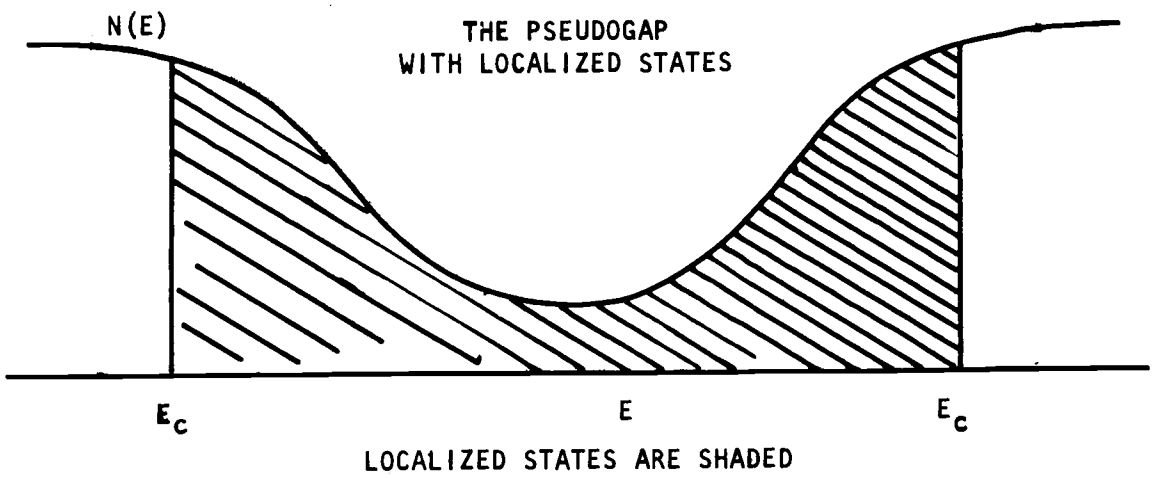

Figure 14. The pseudogap with localized states.

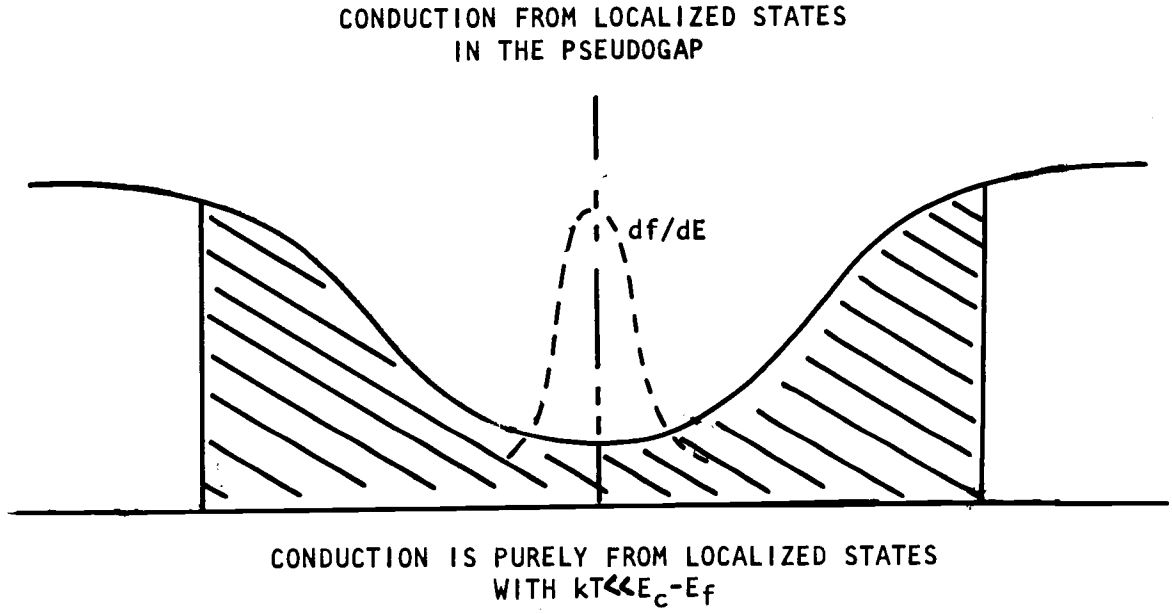

Figure 15. Conduction from localized states in the pseudogap.

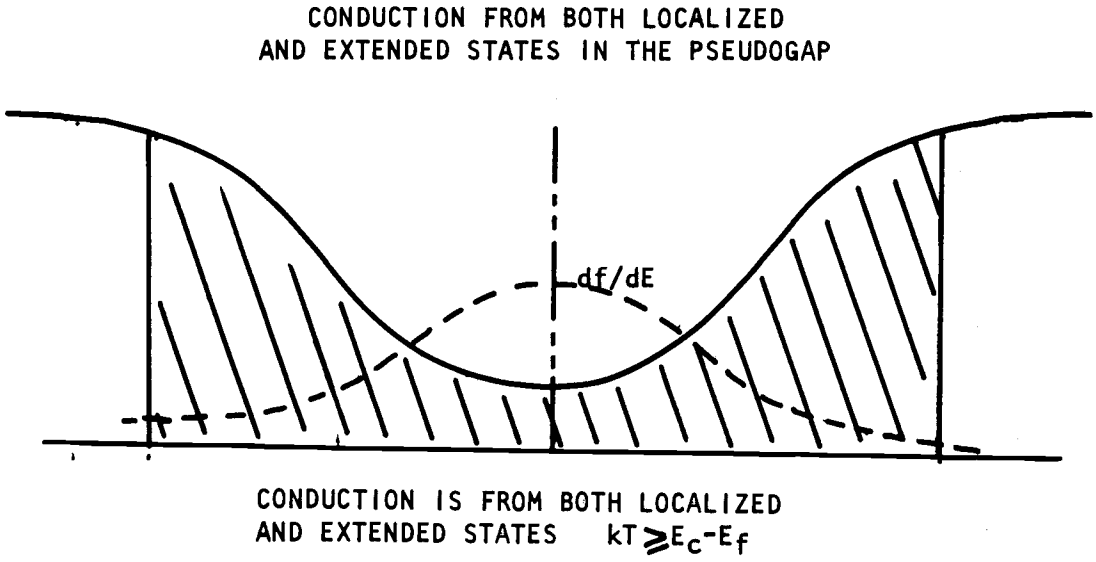

Figure 16. Condution from both localized and extended states in the pseudogap.

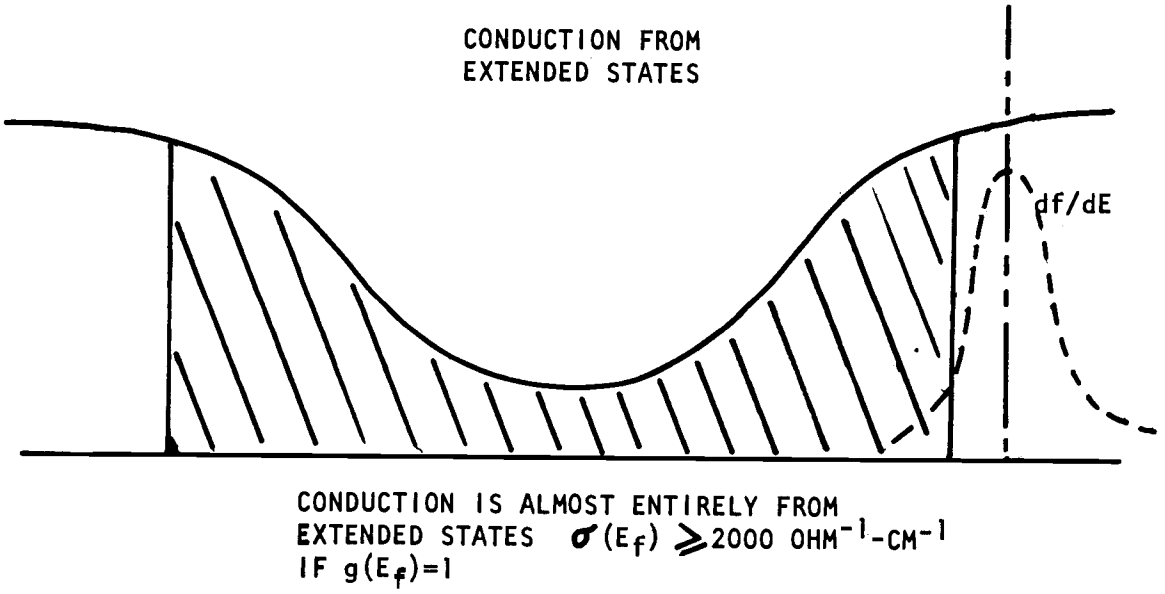

Figure 17. Conduction from extended states.

$$\sigma = \sigma(E_f)_{localized} + \sigma(E_c)_{extended} \exp(E_f - E_c)/kT. \quad (1)$$

$$\frac{\sigma_{localized}}{\sigma_{extended}} \approx 10^{-2} . \quad (2)$$

Since $\sigma(E_c) \approx 100$ ohm^{-1}-cm^{-1} and the lowest experimental values of σ in Tl-Te are not much less than this, it is evident that localized states cannot contribute appreciably to transport in Tl-Te. Therefore we need concern ourselves only with diffusive transport by non-localized electrons.

Transport Theory. The usual Boltzman theory for transport of electrons in conductors has it that the current is given by

$$j = \int nev \, d^3k \quad (3)$$

where j is the current density, e the electron charge, v the velocity and n the distribution of filled states. The integration is taken over momentum space d^3k. An expression for the conductivity is then given by

$$\sigma = \int \vec{v}\vec{v} \, e^2 \tau df^o/dE d^3k \qquad \text{(ref. 11)} \quad (4)$$

In this expression, σ is the conductivity tensor, f^o is the unperturbed fermi distribution function, τ is the scattering time.

These formulas presuppose the scattering length λ is such that $\lambda k \gg 1$, where k is the wave number. All of this is appropriate for most cases of conduction in crystals.

When crystalline order is destroyed, the scattering length of electrons often is reduced to a value comparable to the interatomic distance: $k\lambda \approx 1$, and ordinary transport theory no longer applies. In this case, the electronic wave function no longer has a well defined wave number, and the usual Boltzman expression for conductivity must be replaced by an expression, such as the Kubo expression, which takes into account the short scattering length of the electron.

The Kubo equation for conductivity is

$$\sigma_{ij}(\omega) = \frac{1}{KT} \int_0^\infty e^{-i\omega\tau} d\tau \; < \int i_j(\vec{\xi}, -\tau) i_i(\vec{0}, 0) d\vec{\xi} > \qquad (5)$$

where i is the current operator, $\vec{\xi} = \overrightarrow{x-x'}$, $\tau = t-t'$, and ensemble averaging is denoted by $< >$.

In the Kubo equation, the diadic for velocity $\vec{v}\,\vec{v}$ is replaced by a correlation function using the current operator. When a magnetic field is applied, off-diagonal elements appear in the Kubo tensor for conductivity, and they are proportional to the magnetic field, thus yielding a Hall mobility (see Equations 27, 28).

Transport Theory with Mention of Tl-Te. The theory of Mott (11) can be used to explain some of the electronic behavior shown in

disordered systems. The Mott theory predicts that the normally seen conduction band in mercury be replaced by a pseudogap in which the density of states is reduced from its ordinary value with the increase of interatomic distance, as would be found in mercury taken past its critical temperature. If localization occurs, $(g < 1/3)$, transport will come from electrons excited from the edge of a valence band to the edge of a conduction band (see Figure 16). Contributions from localized states will be masked by contributions from extended states, and the sample will show semiconducting behavior.

$$\sigma = \sigma_o \exp(E_f - E_c)/kT , \quad (\sigma_o \sim 200 \text{ ohm}^{-1}\text{-cm}^{-1}). \qquad (6)$$

For interatomic separations for which localization is precluded, $1/3 < g < 1$, transport will be diffusive, and Mott's theory has the conductivity proportional to g^2:

$$\sigma = S_f e^2 a g^2 / 12\pi^3\hbar, \quad \text{or} \quad \sigma = g^2 e^2/3ha . \qquad (7)$$

(S_f is the fermi area, and the scattering length is a, the interatomic distance.) These formulas are the same as Ziman's for weak scattering, except that the factor g^2 is introduced, and the interatomic spacing replaces the scattering length.

Mott's theory is supported by experiments done on non-dense mercury by Schmutzler and Hensel (12). Schmutzler et al. measure

the conductivity and Seebeck coefficient of non-dense mercury taken past its critical temperature. For densities above 9 g/cm^3 the conductivity and thermopower change slowly with temperature, and for lesser densities the conductivity reduces in magnitude and shows a strong temperature activation, indicating localization. The transition occurs at an interatomic spacing close to that predicted by Mott and the conductivity at the transition point is close to that value predicted by Mott ($\sigma \sim 200$ ohm^{-1}-cm^{-1}). For atomic separations in which Mott's theory would predict diffusive transport ($.3 < g < 1$), the conductivity shows itself to be proportional to g^2 (Equation 7).

$$\sigma \propto g^2 . \qquad (8)$$

Further evidence supporting Mott's theory is provided by the NMR experiments by Warren (13) in which the Knight shift in In^{115} in In_2Te_3 is measured as a function of temperature in the range $800°C < T < 1400°C$. g is calculated from the Knight shift[2] and the degree of localization is inferred from the ratio $\eta = \tau_e/\tau_o$ [3]

---

[2] The Knight shift K is given by $K = 4/3\pi(\gamma_e h)^2 |\psi(0)|^2 gN(E_f)_{fe}$, where γ_e is the electron gyromagnetic ratio, and $\psi(0)$ is the electronic wave function at the nucleus and $N(E_f)_{fe}$ is the density of states for free electrons.

[3] τ_e is the correlation time for spin-spin relaxation. It is also the time the localized electron stays on the atom. $\frac{\tau_e}{\tau_o} = \frac{1/T_1}{1/T_{1(\text{Korringa})}}$. τ_o is the corresponding time for a free electon. $1/T_1$ is the line width, $1/T_{1(\text{Korr})}$ is the free electron line width.

In the experimental temperature range, g goes from a value near zero at the low temperature to a value near one at the high temperature. At the value $g = 1/3$, η changes abruptly an order of magnitude, indicating localization. For the values of g in which diffusive transport would be expected, the conductivity is proportional to g^2, and the correlation time for localized electrons is the scattering time, as would be expected for diffusive transport: $\eta\sigma = \text{constant}$ [4]. Warren found this equation to be valid only for $\sigma \lesssim 2500\ \text{ohm}^{-1}\text{-cm}^{-1}$, which supports Mott's estimate for the upper limit to the diffusive range.

Measurements by Cutler and Field (6) of the thermopower and conductivity of n-type solutions of thallium-tellurium support Mott's description for a two band model of liquid semiconductors. Cutler and Field showed that theoretical equations for the dependence of σ and S on the electron density are obeyed very accurately for Tl_xTe_{1-x} with $x > 2/3$ if $\sigma(E) \propto E$. This would be expected according to Mott's formula, which can be written

$$\sigma(E) \propto \{N(E)\}^2$$

if $N(E)$ has the usual half-power dependence on the energy near a band edge. More recent work by Cutler (unpublished paper) shows

---

[4] $\sigma = e^2N(E)a^2/\tau_e$, for diffusive transport.

also that the effect of temperature on σ and S in this composition range can be predicted quantitatively in terms of a model for the pseudogap.

Theory of Hall Measurements

Random Phase Model. The random phase model is especially suited for treating electronic transport in disordered systems, where the scattering length is comparable to the interatomic distance, and the wave functions have poorly defined momenta.

Hindley (14) uses random phase wave functions, which are extended wave functions, suitable for disordered systems. The desired non-localized wave functions $|k>$ are a linear combination of atomic orbitals, $\phi_m(r-R_n)$.

$$|k> = \sum a_{nk}\phi_n(r-R_n) \; . \qquad (10)$$

The ϕ_n are atomic orbitals (such as Wannier functions) and the a_{nk} are coefficients whose phases vary in a random way from atomic site to atomic site, but whose amplitudes are approximately equal for all sites. They are suitable for describing the random phase scattering process and they yield a uniform probability distribution for electrons over all atomic sites.

$\langle |a_{nk}|^2 \rangle_c = 1/NV$ where $\langle \rangle_c$ represents ensemble average over configurations, V is the volume of the system, and $N = a^{-3}$ is the number of atoms per unit volume, a being the interatomic spacing. (The value $1/N$ is what would be expected for the diagonal elements of a density matrix for a completely random system.)

The result of any general expression for an operator, using the RPM is

$$\langle |\langle k'|A|k\rangle|^2 \rangle_c = (\frac{a^3}{V}) \langle \sum_{n'} |\langle n'|A|n\rangle|^2 \rangle_c + \langle [\langle n|A|n\rangle]^2 \rangle_c \delta_{kk'} \tag{11}$$

These are used in the Kubo expression for conductivity.

Transport Theory. We have given earlier in this discussion an expression from Boltzman theory for the conductivity tensor.

$$\sigma = \int \vec{v}\,\vec{v}\, e^2 df^o/dE\, d^3k\,, \tag{12}$$

where the terms mean the same as before. For the simple case of isotropic scattering $(\tau(k) = \tau)$, and cubic symmetry, the conductivity tensor appears as:

$$\sigma = ne \begin{bmatrix} e\tau/m & 0 & 0 \\ 0 & e\tau/m & 0 \\ 0 & 0 & e\tau/m \end{bmatrix} \tag{13}$$

We see that $\sigma_{xx} = \sigma_{yy} = \sigma_{zz} = ne^2\tau/m$, $\sigma_{ij} = 0$, $i \neq j$.

When a magnetic field is introduced in the sample, the conducting electrons have a Lorentz force exerted on them, and, because of it, the current is deflected in the direction different from the direction of the applied electric field. Then the conductivity tensor has non-zero off-diagonal elements. For the case of $\vec{E} = E_y$, $\vec{H} = H_x$ (cubic symmetry and isotropic scattering still applying), the diagonal elements become:

$$\sigma_{xx} = \int \frac{v_x^2 e^2 \tau df^o/dE\, d^3k}{1+e^2\tau^2H^2/m^2} \tag{14}$$

and the off-diagonal elements are:

$$\sigma_{yz} = \frac{1}{m} \int \frac{v_x^2 e^3 \tau^2 df^o/dE\, d^3k}{1+e^2\tau^2H^2/m^2} \tag{15}$$

For the case of weak magnetic field $(e^2\tau^2H^2/m^2 \ll 1)$ and isotropic scattering, the conductivity tensor, in the presence of a magnetic field becomes

$$\sigma = ne \begin{bmatrix} e\tau/m & 0 & 0 \\ 0 & e\tau/m & e^2\tau^2H/m^2 \\ 0 & -e^2\tau^2H/m^2 & e\tau/m \end{bmatrix} \tag{16}$$

The Hall coefficient R derives from the fact that transverse surfaces of a finite sized conductor collect electrons which set up an electric field (the Hall field) which returns the deflected current to its original unperturbed direction.

$$R = \sigma_{xy}/\sigma_{xx}^2 \cdot 1/H \; . \tag{17}$$

$R = 1/ne$ for the nearly free electron approximation.

In the case of strong scattering, where transport is diffusive, with scattering length comparable to interatomic distances, the Kubo formula for conductivity (either in or out of a magnetic field) is used. A salient difference between the Kubo formula, and any formula derived from Boltzman scattering theory lies in the difference in definition of "velocity." For the Boltzman theory (weak scattering) velocity is equal to the derivative of the expression for energy with respect to momentum. For strong scattering, the strongly localized wave functions do not permit an easy definition of velocity. Velocity in the Kubo equation is taken as the commutator of position with the Hamiltonian.

The Kubo equation:

$$\sigma_{ij} = e^2 \hbar [F_{ij}(\Omega) - F_{ij}(0)] \tag{18}$$

where

$$F_{ij}(\Omega) = \int_0^{\beta} du \exp(\hbar\omega u) \frac{1}{Z} Tr\{\exp(-H(\beta-u))v_i \exp(-Hu)v_j\} \qquad (19)$$

$\beta = 1/kT$, Ω is a complex variable and the integration is carried out in the complex plane. The expression with v_i and v_j is a velocity correlation function, and is analogous to the velocity diadic in the Boltzman expression (Equation 12). Taking the trace of the product of the correlation function tensor with the density matrix gives the (orientation) ensemble average. Z is the thermodynamic partition function.

The electrical conductivity is obtained by evaluating the diagonal elements of the Kubo tensor. We set $i = j$ so that

$$\frac{1}{Z} Tr\{\exp(-(\beta-u)H)v_x \exp(-uH)v_x\}$$

$$= \frac{1}{Z} \sum_{\chi} \exp(-\beta\epsilon_{\chi}) \sum_{\chi'} \exp(u(\epsilon_{\chi}-\epsilon_{\chi'}))|\langle\chi|v_x|\chi'\rangle|^2 . \qquad (20)$$

From before, (Equation 11) where we learned

$$\langle|\langle\chi|v_x|\chi'\rangle|^2\rangle = \frac{a^3}{V} \sum_{n'} |\langle n|v_x|n'\rangle|^2 \qquad (21)$$

(using the random phase model), Friedman (15) gets, after carrying out the indicated integration:

$$\mathrm{Re}\langle\sigma\rangle = \frac{2\pi}{3}\left(\frac{e^2}{\hbar a}\right) z a^6 J^2 [N(E_f)]^2 \quad . \tag{22}$$

Here a is the interatomic distance, z is the coordination number, J is the interaction integral between atomic sites, and $N(E_f)$ is the density of states at the fermi energy. This result is in agreement with those of Mott and Hindley (10, 14).

To show the dependence of the off-diagonal elements on the magnetic field, an expansion to third order in the magnetic field dependent transfer integrals must be made. After performing the indicated averaging and summations, the terms containing the magnetic field dependence:

$$\langle\chi|v_x|\chi'\rangle\langle\chi'|\Delta H|\chi''\rangle\langle\chi''|v_y|\chi\rangle \tag{23}$$

can be written in terms of localized wave functions as:

$$\left(\frac{a^3}{V}\right)^2 \sum_{m',n'} \langle m|v_x|m'\rangle (J^{(H)}_{m'n''} - J^{(0)}_{m'n''})\langle n''|v_y|m\rangle \tag{24}$$

where J is the interaction strength between localized sites, expressed as an overlap integral.

$$J^{(H)}_{n'n} = J^{(0)}_{n'n} \exp(i\alpha_{n'n}), \tag{25}$$

where

$$\alpha_{n'n} = e/hc \cdot H \cdot \frac{1}{2} nXn' \quad .$$

$H \cdot \frac{1}{2} nXn'$ is the magnetic flux through the origin and sites n' and n. This identity is used in the expression for the antisymmetric part of the correlation tensor:

$$F_{xy}^{(a)}(\Omega) = \frac{1}{2}[F_{xy}(\Omega) - F_{yx}(\Omega)] \tag{26}$$

to yield:

$$\sigma_{xy}^{(a)} = \frac{8\pi^2}{3} \frac{e^2}{\hbar} \left(\frac{eHa^2}{\hbar c}\right) a^8 J^3 \bar{z}[N(E_f)]^3 \tag{27}$$

An expression for the Hall angle in which the Kubo expression is used is:

$$\theta_H = \frac{\sigma_{xy}}{\sigma_{xx}} = 4\pi(eHa^5/\hbar)JN(E_f) \cdot f \tag{28}$$

In this expression, θ_H is the Hall angle, H is the magnetic field, J is the interaction integral, a is the interatomic spacing, and $N(E_f)$ is the density of states at the fermi energy. $f \sim 1$, depending on the coordination number. The Hall mobility μ_H is obtained from $\mu_H = \theta_H/H$.

What Our Measurements Imply in Relation to Current Theory

Friedman's calculations use the Random Phase Model to yield expressions for the conductivity and Hall mobility (15). The RPM is especially appropriate to liquid semiconductors, such as ours, where conductivity is in the range for diffusive transport. We therefore

compare our measurements to Friedman's calculations.

First of all, our disordered system has the conductivity of the right magnitude ($400\ \text{ohm}^{-1}\text{-cm}^{-1} < \sigma < 1000\ \text{ohm}^{-1}\text{-cm}^{-1}$) to indicate non-localized, strong scattering conduction. At compositions far away from intrinsic, our measurements yield a value of $\mu_H \approx 0.1\ \text{cm}^2/\text{v-sec}$, the same as that estimated by Friedman. On the thallium-rich side of intrinsic composition, both the Hall mobility and conductivity are temperature independent, which is in accordance with Friedman's calculations. Any temperature dependence of μ_H would reside in $N(E_f)$ at these compositions, but E_f is independent of temperature in the degernerate statistics which characterize these compositions (Equation 28).

On the tellurium-rich side of intrinsic composition (p-region) the Hall mobility μ_H is independent of temperature, but the conductivity shows a strong temperature dependence. These results are at variance with Friedman's calculations. Friedman's expression for conductivity (Equation 22) has the conductivity proportional to the square for the energy density of states. The fact that σ changes strongly with temperature in the p-region implies that $N(E_f)$ changes strongly with temperature, according to Friedman. Consequently, according to Equation (28), $\mu_H = \theta_H/H$ should be proportional to $N(E_f)$ and should have the same temperature dependence as $\sigma^{1/2}$. This is not observed.

At intrinsic composition, μ_H shows a moderate temperature dependence, in contrast to its behavior at the extrinsic compositions. This behavior could be explained by a two band model in which the relative populations of holes (with $\mu_H = 0.4$ cm^2/v-sec) and electrons (with $\mu_H = 0.1$ cm^2/v-sec) change with temperature:

$$\mu_H = \frac{\sigma_n \mu_n + \sigma_p \mu_p}{\sigma_n + \sigma_p} \tag{29}$$

In conclusion, measurements have been made of the conductivity and Hall mobility of liquid solutions of thallium-tellurium, in compositions ranging from pure tellurium to 69.0 atomic percent thallium. At compositions on the thallium-rich side of intrinsic composition, both the conductivity and Hall mobility are temperature independent, and the data can be explained by existing theories pertinent to diffusive transport in disordered systems. On the tellurium-rich side of intrinsic composition, the Hall mobility is temperature independent whereas the conductivity shows a strong temperature dependence. This behavior is at variance with the theory most relevant to liquid thallium-tellurium mixtures. At intrinsic composition, the Hall mobility shows a moderate temperature dependence, and the data can be explained in light of a two band model.

BIBLIOGRAPHY

1. A.F. Ioffee and A.R. Regel, Prog. in Semiconductors, 4, 239. 1960.

2. M. Cutler and C.E. Mallon, Phys. Rev., 144, 642 (1966)

3. A.J. Greenfield, Phys. Rev., 135, 1589-95 (1965)

4. B.T. Kolomiets, Phys. Stat. Sol., 7, 714-31 (1964)

5. A.H. Clark, Phys. Rev., 154, 750-757 (1967)

6. M. Cutler and M.B. Field, Phys, Rev., 169, 632-41 (1968)

7. W.W. Warren, Phys. Rev., B6, 2522 (1972)

8. J.E. Enderby and C.J. Simmons, Phil. Mag., 163, 125 (1969)

9. P.W. Anderson, Phys. Rev., 109, 1492 (1958)

10. N.F. Mott, Phil. Mag., 17, 1259 (1968)

11. J.M. Ziman, Electrons and Phonons

12. R.W. Schmutzler and F. Hensel, Ber. Bunsenges. physik Chem., 76, 531-5 (1972)

13. W.W. Warren, Jr., Journal of Non-Crystalline Solids, 4, 168-77 (1970)

14. N.K. Hindley, Journal of Non-Crystalline Solids, 5, 17-30 (1970)

15. L. Friedman, Journal of Non-Crystalline Solids, 6, 329-41 (1971)

16. J.E. Enderby and L. Walsh, Phil. Mag., 991 (1966)

17. R.S. Allgaier, Phys. Rev., 185, 227 (1959)

APPENDICES

APPENDIX A

The Hall Cell

The general shape of the Hall cell has already been described in the General Method section. A more detailed description will be given here.

Both the plates used in the cell have dimensions 1.0" x 2.0" x .12". The channel has dimensions 1.5" x .25" x .003" and is cut in the plate by a Cavetron ultrasonic rectangular cutting tool. The 0.003" figure is nominal, and accurate measurement shows it to be 0.00421 ± 0.0003 inches deep. Accurate measurement is done by an instrument called a Sherr depth gauge which measures depths and thicknesses to within one hundred thousandth of an inch. The gauge has a needle-like stylus which probes a surface to given readings of depth. For the measurement of the channel, the stylus is caused to probe across the face of the plate, dip down into the depth of the channel, measure across the width of the channel, and finally rise up the bank on the other side of the channel.

A triangular set of probe holes in the tube plate meets the channel (when the two parts of the cell are clamped together) in a way shown in Figure 18. If the three holes met the channel exactly on its banks, then the expression for the Hall coefficient would be given by:

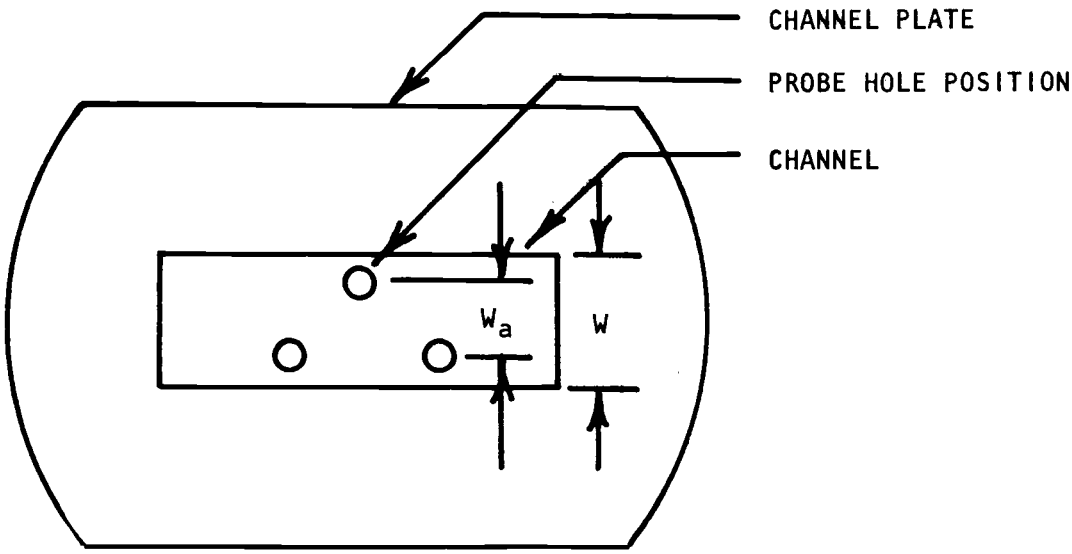

Figure 18. Channel plate.

$R_H = Vt/BI$ where V is the Hall voltage across the entire width of the channel, t is the depth of the channel, B is the strength of the magnetic field, and I is the magnitude of the current. However the width over which the Hall voltage is measured is W_a, not W, and so elementary considerations show that R_H should be given by: $R_H = V_H tW/BIW_a$ where V_H is the Hall voltage measured by the probes.

The ratio W/W_a is found by placing the tube plate and channel plate on an overhead projector producing a magnified image on the wall. The image can then be measured easily with a ruler.

APPENDIX B

Clamping Arrangement and Electrical Lead Outs

During a data run, it is necessary for the channel plate to be clamped firmly to the tube plate. At the same time, the graphite pucks must be pressed firmly to the probe holes, and electrical contact made between the sample and lead out wires. All of this is accomplished with parts called the rack, the arbors, and the palette (see Figures 20, 21 and 22).

The rack, as shown in Figure 21 is made of molybdenum and consists of two rails 4" x 3/8" x 3/16" riveted at right angles to two molybdenum ties 1-1/2" x 3/4" x 1/16".

The arbors, as shown in Figure 22, are made of molybdenum and are omega shaped. They each have two 1/8" holes drilled through them to allow passage of spring loaded bolts.

The palette, as shown in Figure 20 is made of stoneware. It is formed by molding moist and pliable stoneware (name for a feldspar clay that potters use) into an aluminum breakaway mold. After the palette is removed from its mold, it is allowed to dry and then is fired until it reaches suitable strength. Holes are drilled in a fired sample of stoneware with a silicon carbide twist drill, and finishing trimming is done with a diamond studded glasscutting saw. Molybdenum leaf springs with attached platinum lead-out wires (Figure 19)

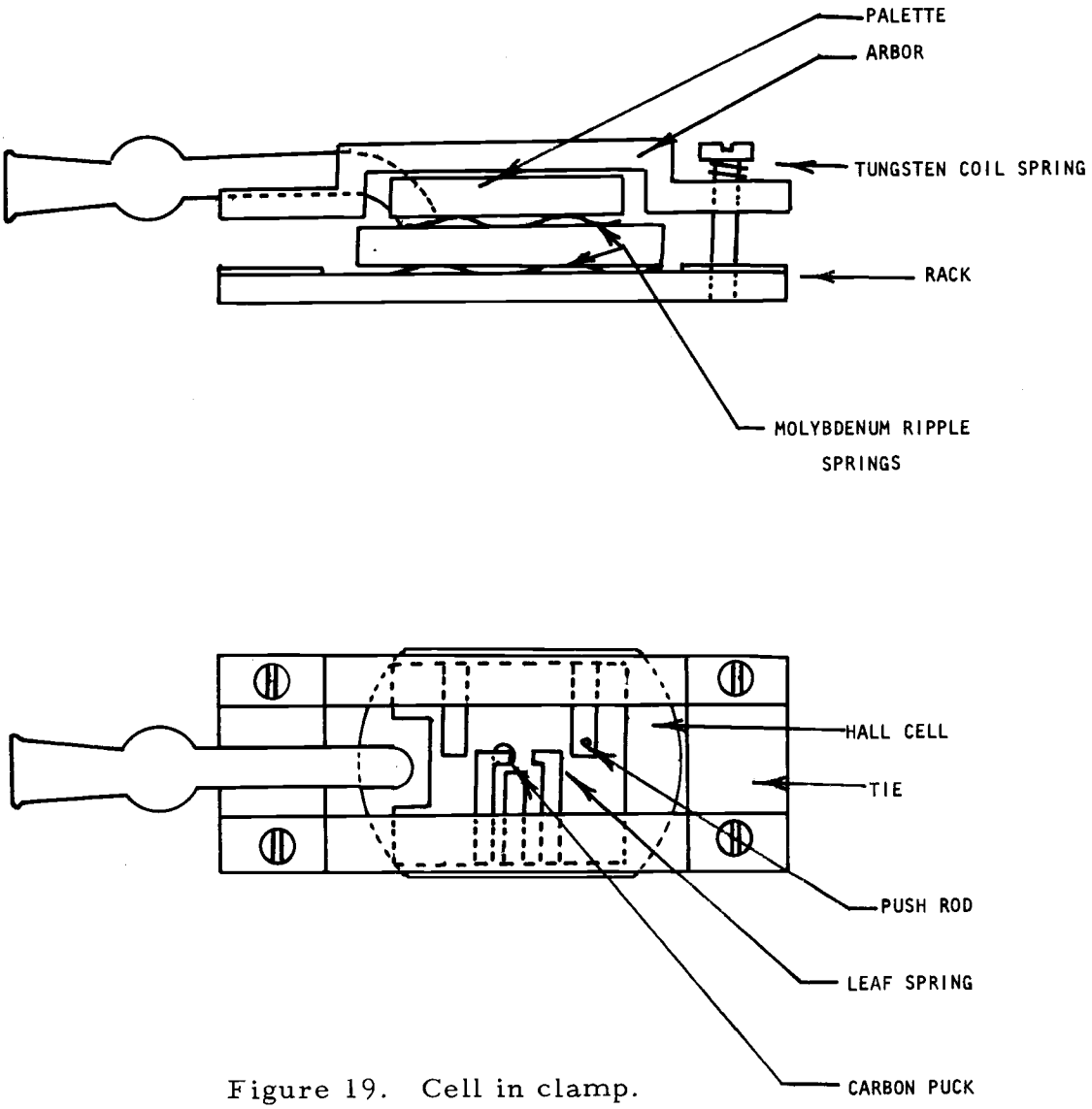

Figure 19. Cell in clamp.

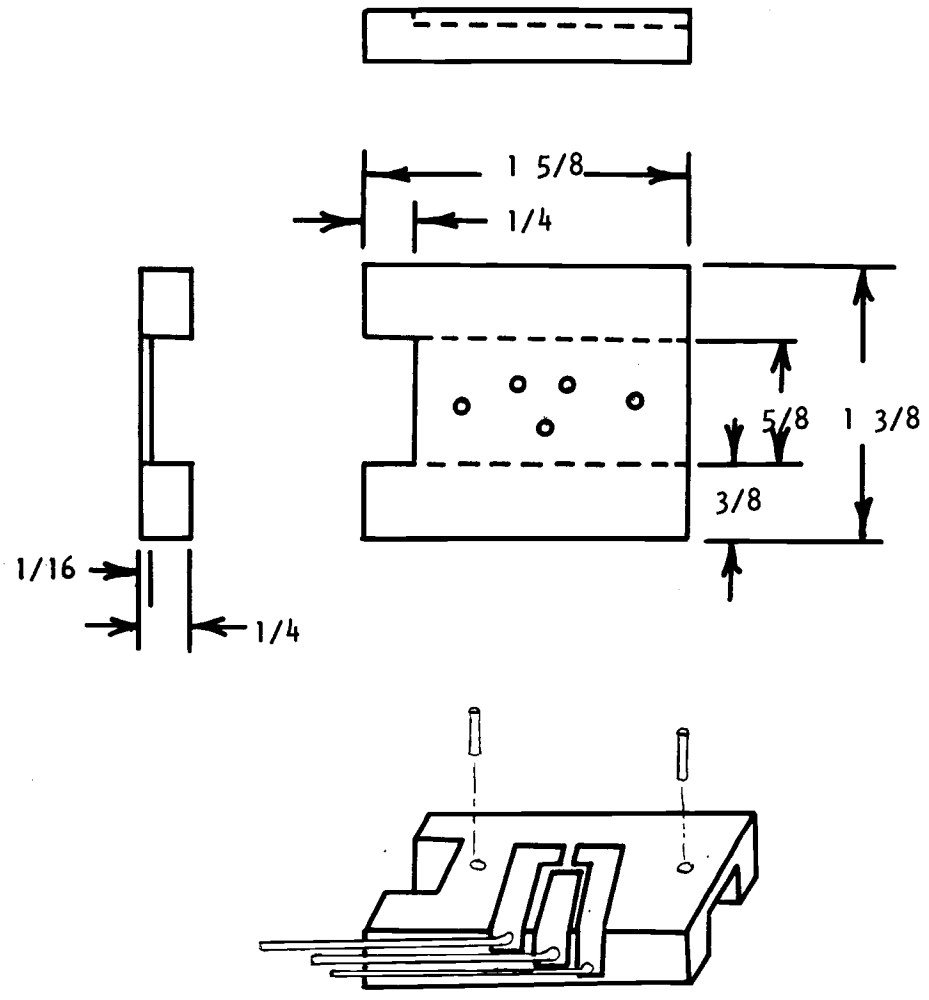

Figure 20. Palette.

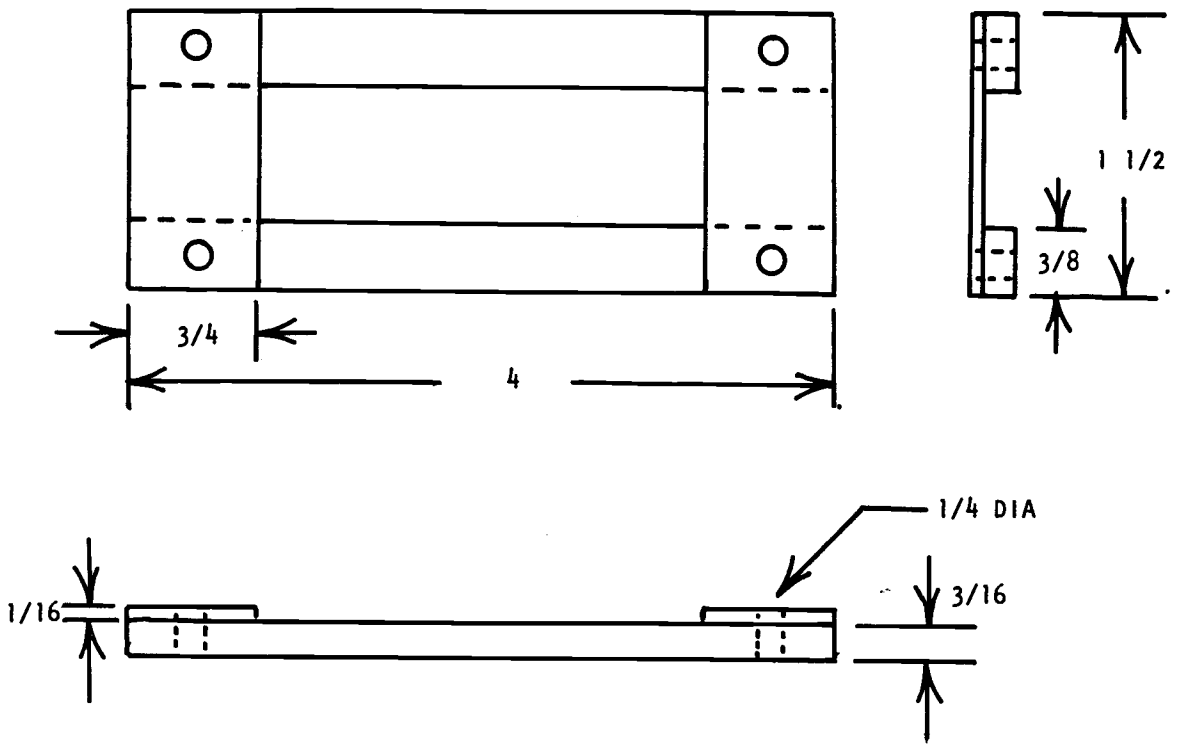

Figure 21. Rack.

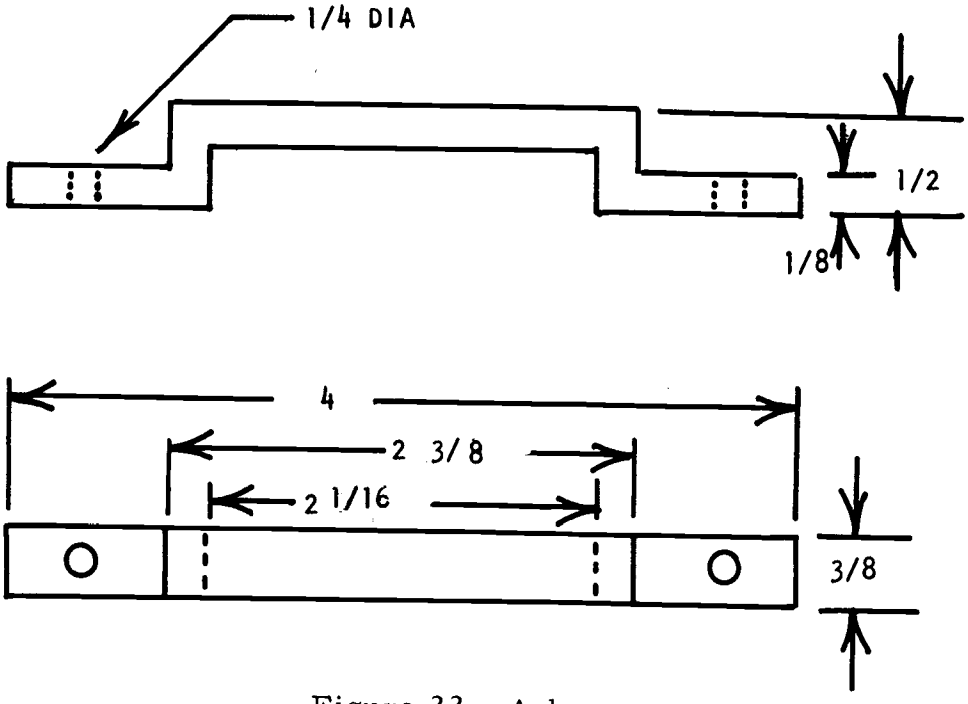

Figure 22. Arbor.

are separately fashioned and their tails are anchored to the edges of the palette with Avco MV 30 cement. The heads of the leaf springs are each positioned over 1/16" holes drilled in the palette, drilled in a way such that when 1/16" molybdenum push rods are put in the holes, the heads of the leaf springs will cause the push rods to press against the pucks. The pucks are each over a probe hole.

When clamping is to be done, as shown in Figure 19, the arbors press against the leaf springs and the leaf springs exert pressure on the pucks via the push rods. In this way the pucks are held in position by the push rods. When the Hall cell is to be clamped, the bottom surface of the channel plate of the cell is placed on molybdenum ripple springs resting on the tracks of the rack and the top surface of the tube plate is pressed against molybdenum ripple springs set on the outer edge of the palette, as shown in Figure 19. The arbor presses down the palette against the ripple springs, the points of contact including the bases of the leaf springs. The pressure on the pucks is maintained by the bending of the leaf springs caused by the fact that the push rods displace the heads of the leaf springs in the final position.

The ripple springs are made by pressing thin strips of molybdenum metal between corrugated "Dutch nails" used in the construction of screen doors. The tungsten coil springs are made by winding 0.040" tungsten wire around size 10 bolts. In order to reduce the

chance of breakage, heat is applied to the spring while it is being wound.

The cell and accompanying clamping arrangement, as shown in Figure 19, are supported by molybdenum rods which bolt into the ties near the center of the envelope. The (relatively) cool ends of the rods go into alundum sleeves which are supported by brass rods which go into the aluminum headstock and tailstock pieces, shown in Figure 23. This arrangement is essential to reduce the heatflow along the molybdenum support rods; it makes it possible to keep the cell at the furnace temperature.

Electrical Lead-Outs

There are two current-bearing wires leading up to one side of the Hall cell palette. They are in the form of a coaxial cable in order to minimize magnetic pickup to the probes. The "lead-in" current-bearing wire is contained in a thick walled ceramic tube which in turn is contained in a stainless steel tube whose body serves to conduct the "lead-out" current. At the point where the current bearing tube reaches the arbor of the cell, the coaxial arrangement is abandoned (because of space limitations) and the two current-bearing wires are cemented to an arbor and one side of the palette. They are ultimately spot welded to the tails of the current-bearing leaf springs.

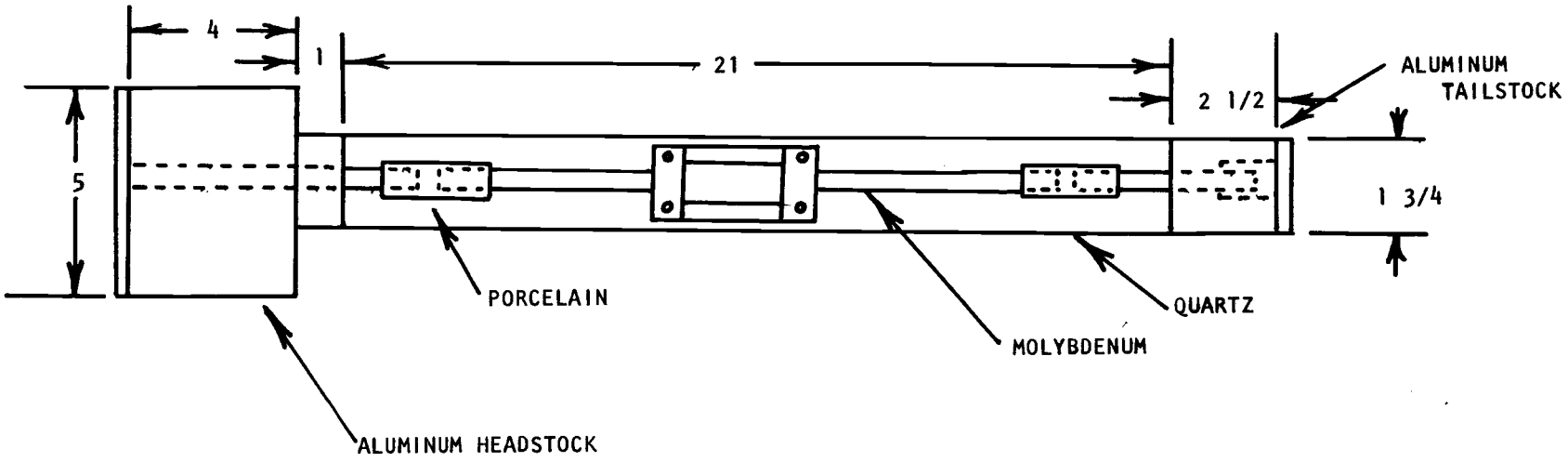

Figure 23. Quartz envelope.

There are three signal-bearing wires leading up to the other side of the Hall cell palette. All three wires are contained and insulated from one another in a multibore ceramic tube. The tube terminates at the palette and the signal bearing wires are spot welded to the tails of the molybdenum leaf springs which go to the probes. Both the current and the signals reach the pucks via molybdenum push rods which are held by the leaf springs.

All of the lead-out wires pass out of the envelope into the room atmosphere via Stupikoff seals in the aluminum bulkhead.

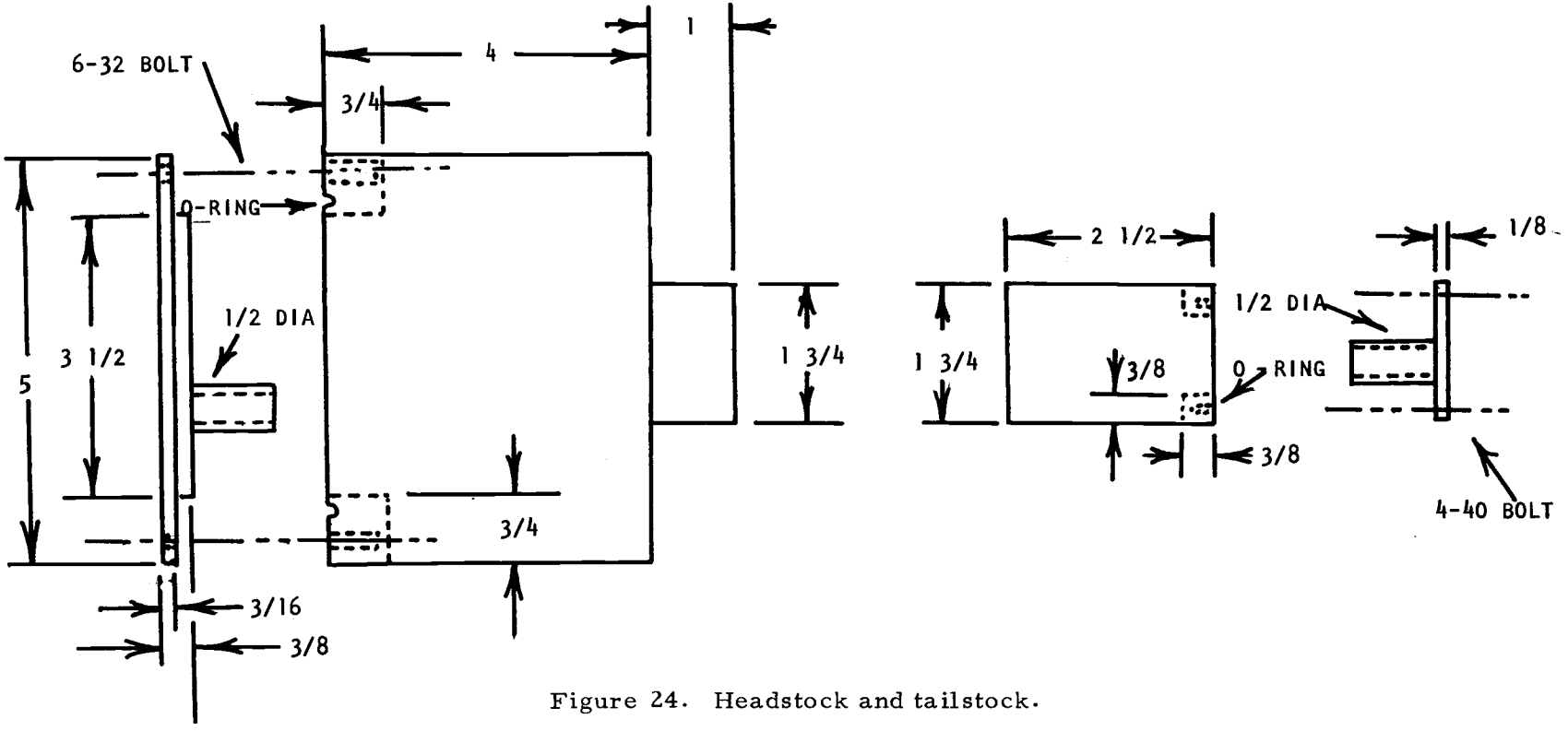

Figure 24. Headstock and tailstock.

APPENDIX C

Preparation of Samples

Pure thallium tarnishes in room atmosphere and so special measures have to be taken to remove the oxide from a stick of thallium that has been exposed to room atmosphere. A slug of the metal is put into a pyrex tube resting inside a pyrex envelope containing argon. If a mixture containing tellurium and thallium is desired, a test tube containing a weighed amount of tellurium is placed at the lower end of the tube containing the thallium. (This too is in the envelope containing argon.) The thallium slug is heated past its melting point and allowed to run down its cleaning tube containing the tellurium. The oxide remains behind, sticking to its pyrex tube. When the oxide-free thallium drains into the test tube of tellurium, the test tube is heated and agitated. The exact composition of the mixture can be ascertained from the increase in weight of the contents of the test tube since all of the increase can be attributed to the addition of pure thallium. It was discovered that samples of 31 atomic percent (X31) drop out of their test tubes easily and do not tarnish in room atmosphere. Since tarnishing does not occur for this mixture it can be pulverized in order to counteract the effects of phase segregation during solidification and handled in room atmosphere with ease; similarly for X45, X48, and X60.

A slug of X70 (n-type) was prepared in the manner described for the p-type samples. The large ingot that resulted tarnished in spots on its surface and so it was considered risky to pulverize the sample. Pulverization would expose enormous amounts of surface area to tarnishing and the sample would be ruined. The large ingot was put into a quartz tube (1" diameter) with a smaller tube (1/8" diameter) running down its inner wall. The open end of the quartz tube has a one-hole stopper and bellows arrangement attached to it which allows a ladle to slide down into the bottom of the tube. The lower end of the quartz tube is heated red hot and argon from the small diameter tube bubbles through the material of the large ingot (which is liquid from the heating). The high temperature assures that the sample is completely liquid and the vigorous bubbling from the argon assures that the sample is uniform. The cup of the ladle is made from stoneware coated with alundum cement. Both these materials retain their strength at high temperaturea and the alundum cement coating prevents the sample from wetting the cup. As a result, the solid little ingot which forms on cooling drops out of the cup nicely.

The term X70 is a nominal term for a mixture whose composition was very accurately determined to be 70.85 ± .01. (The ingredients of a 10 gram sample can be weighed to within 0.1 mg.) Other samples with less thallium were made by adding accurately weighed

amounts of tellurium (typically 40.0 mg ± 0.1 mg) to accurately weighed amounts of X70.85 (typically 1.000 g ± 0.1 mg). The resulting compositions were accurate to ± .01%.

APPENDIX D

Electronic Circuits and Magnet

The central part of the electronics is the Princton Applied Research lock-in amplifier, as shown in Figure 25. It contains a reference signal oscillator, a phase sensitive detector, a tuned amplifier, a D. C. amplifier-low pass filter combination, and a phase shifter.

In the experiments done here, the reference oscillator drives a power amplifier which sends an A. C. current through the Hall cell and monitoring resistor in series with the cell. In preparation for a run, the voltage signal across the monitor resistor is fed into the signal input of the tuned amplifier and the phase shifter is adjusted so that the relative phase between the signal across the monitor resistor and the signal of the reference oscillator is zero. It is possible that there are voltages other than Hall voltages which are in phase with (or have a component in phase with) the Hall current, and they could be picked up and mistaken as Hall voltages. Other tests have to be made to eliminate or explain that kind of signal. See especially the chapter, Experimental Method.

The magnet has six inch diameter pole faces spaced six inches apart. Its magnetic field is adjustable to any strength up to 5 KG and it can be reversed in direction. It is powered by a regulated power

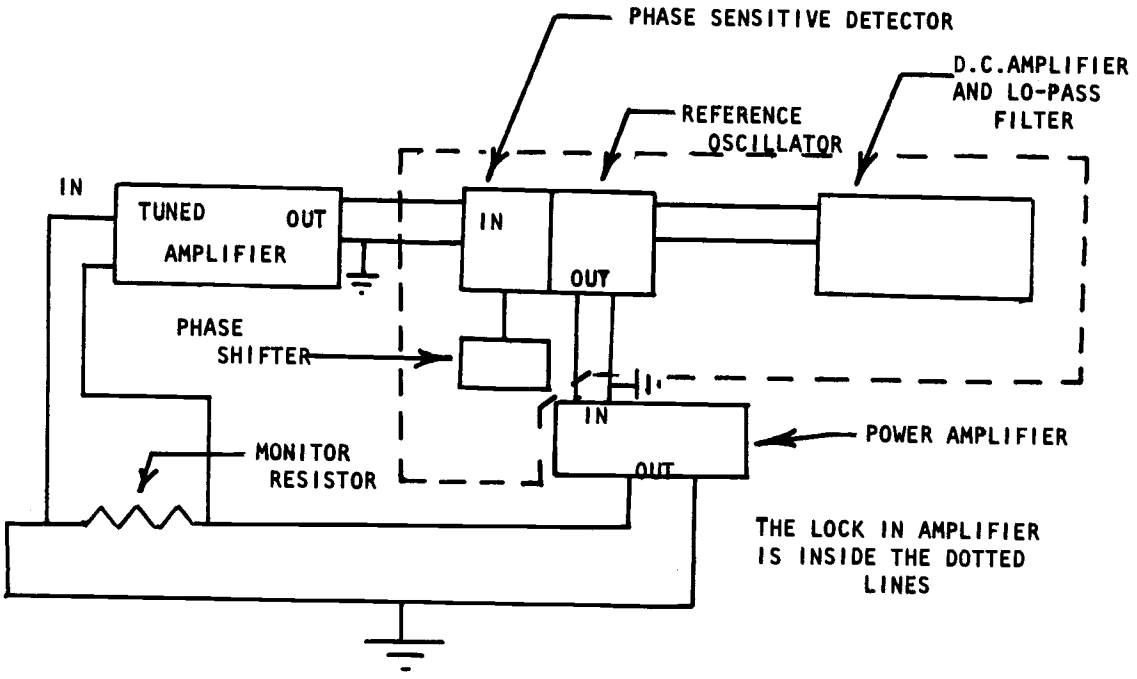

Figure 25. Electronics.

supply which, when the magnet is at its full strength of 5 KG delivers 12 amps at 240 volts. A motor driven powerstat increases the current from 0 to 12 amps in one minute.

The strength of the magnetic field is measured by a gaussmeter.

APPENDIX E

Preparation of Hall Cell for Data Runs

Cleaning the Hall Cell

Both parts of the cell are washed with tap water and dried with the gentle heat of a Bunsen burner. The inner surfaces of the plates are then held together with a piece of lens tissue between them. The tissue is pulled out from between the cells while the cells are still being held together. Any pieces of dust or grit are caught in the tissue in this way and removed from between the cell's inner faces. If the cell's inner faces are made free of dust and grit, then, in the presence of ordinary room light, rainbow patterns appear between the faces, and wide spacing of the fringes indicate absence of grit.

Short narrow strips of masking tape are put on the cell's plate edges to hold the cell together so that it can be clamped together in a brass rack which looks very much like the molybdenum rack used during actual Hall runs.

The pucks are pressed down over the proble holes and a small drop of very dilute airplane glue is used to glue the puck to the cell. Similarly, dilute glue is used to glue the cell plates together. This glue later becomes carbonized during the bakeout process and the remaining carbon helps hold the cell plates together during the Hall

run. The cell is removed from the brass clamp and put into the molybdenum clamping arrangement described in Appendix B.

Bakeout Procedure

The envelope is placed in the tubular furnace and its air is pumped out through a glass tube sealed through the tailstock. Air is also pumped out of the cell through a glass tube sealed through the bulkhead leading into the elbow tube of the tube plate. (There is a male standard tapered joint fitting into the female standard tapered joint of the elbow tube in the tube plate. The male joint is connected to a tube through the bulkhead by a flexible connection.) The bakeout is done in a vacuum in order to remove adsorbed gases.

The Hall Run

After the bakeout is finished, and the cell has cooled to room temperature, the cell and clamping arrangement are removed from the envelope and the solid sample of thallium-tellurium is placed in the elbow tube of the tube plate. Again the cell, clamps, and support are placed in the envelope and hooked up to the vacuum lines just as in the bakeout procedure. Air is pumped out and argon is admitted into the cell and envelope. The furnace is turned on, and when the temperature has risen past the melting temperature of the sample, the whole assembly (envelope, cell and all) is gently rocked back and forth

to stir the sample so that any possible stratification of the liquid in the elbow is broken up. The cell is finally rotated so that the liquid sample rolls from the elbow of the tube plate's tube to the port where the tube enters the channel of the channel plate. The argon gas pressure in the cell tube is then increased enough above the ambient argon pressure of the envelope so that the liquid is forced into the channel. This pressure difference is maintained throughout the entire Hall run.

There is a flow of gas through the envelope during the entire run. A gas flow is necessary to maintain a steady pressure differential between the Hall cell and the surrounding envelope. Details of the gas flow and pressure control system are given in the next subsection.

Gas Flow and Pressure Control System

As shown in Figure 26, the system consists of a bottle of argon set at regulated gauge pressure of about 10 psi, glass stopcock valves, V1, V2, V3, V4, V5, V6, needle valves (can be open and shut smoothly) N1, N2, N3, and vacuum pumps P1 and P2. The Hall cell is shown in the envelope. The cell is not hermetically sealed from the envelope pressure--gas can be forced from the volume of the elbow tube through the minute interstices between cell plate faces into the cell's surroundings. It is a high impedance gas leak, but a leak nonetheless. It is large enough to permit an entering liquid sample to force out all gas in the channel as it enters, but small enough to

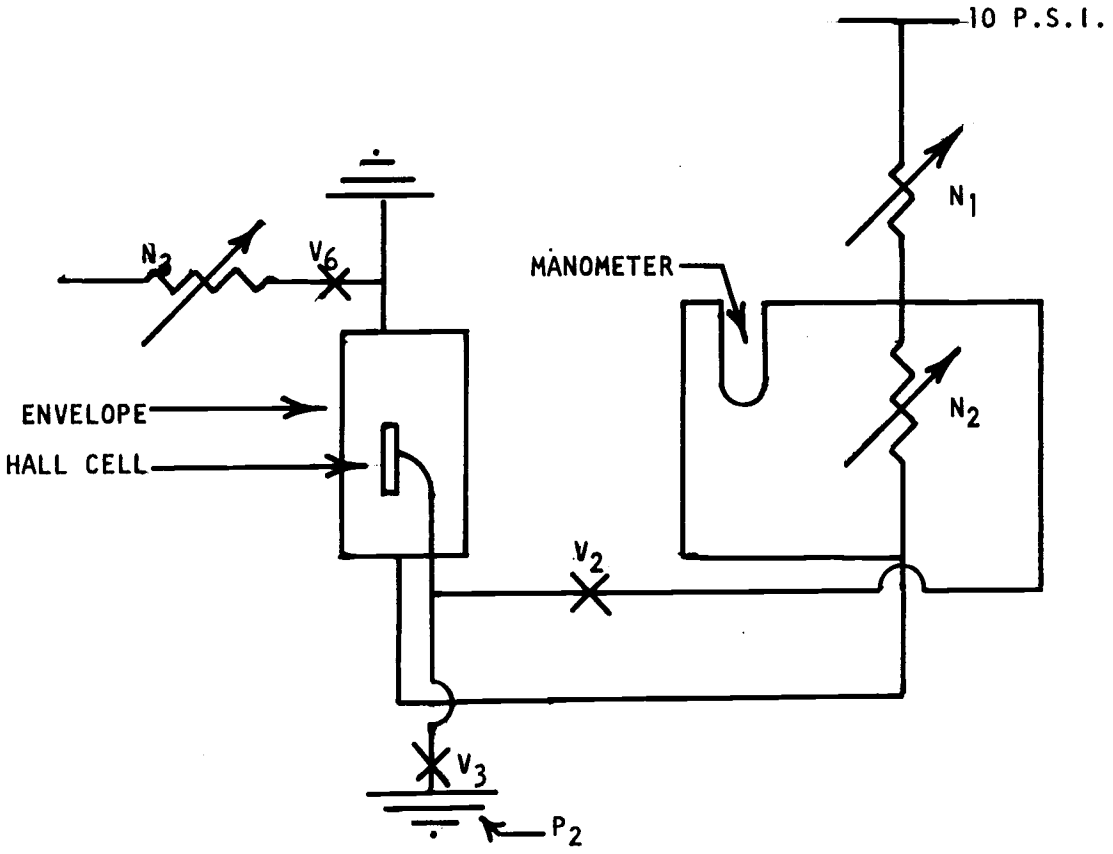

Figure 26. Gas monitoring system.

prevent the liquid sample from leaking out of the channel.

If it is desired to evacuate the envelope and cell, as it would be for bake-out procedure, valve V1 is closed (to cut off gas flow) and valve V6 is closed to atmosphere. Needle valve N2 is opened up, and valves V5, V4, and V2 are opened up. That arrangement allows pump 1 to evacuate the envelope and to evacuate the Hall cell. It is a long route from pump P1 to the Hall cell and this evacuation procedure does not empty the cell very well, but it is a safe procedure because it assures that the cell and envelope will lose pressure at the same rate. The pressure differential is monitored by reference to the mercury manometer M, and if the cell and envelope were to have vastly varying pressures at any given time, the manometer would have its mercury climbing out of control up one or another of its arms. When the cell and envelope are evacuated as well as can be done by the previously described procedure, the cell is pumped out more thoroughly by closing off valve V2 and opening up valve V3. This exposes the cell to pump P2 via a low impedance pumping line and the cell is finally pumped to vacuum high enough to permit it to outgas thoroughly during the bakeout procedure.

In order to admit gas to the cell and envelope, valves V3 and V5 are closed; this cuts off the evacuating action of the pumps. Needle valve N1 and valve V1 are closed, and valve V2 and needle valve N2 opened. Then valve V1 is opened and needle valve N1 is opened

slowly so that gas flows steadily into the cell and envelope. When the envelope and cell reach atmospheric pressure, valve V6 is opened and the gas flows into the atmosphere through a pyrex wool wad designed to trap any vaporized tellurium.

If an above-atmosphere pressure is wanted in the cell and envelope, then needle valve N3 can be turned slightly toward closure to generate an impedance between envelope and atmosphere. If it is desired that the pressure of the cell be raised above the pressure of the envelope, (as it would be for the time when the liquid sample is to be forced from the elbow tube to the channel) then needle valve N2 is turned slightly toward closure to generate an impedance between the cell and envelope. Then the gas flow through valve N2 will generate a pressure gradient between the cell and envelope, and the cell will finally have a higher pressure than the envelope.